No benefits in any form have been received or will be received from a commercial party related directly or indirectly to the subject of this article.

References

1. **Kotz R, Dominkus M, Zettl T, et al.** Advances in bone tumour treatment in 30 years with respect to survival and limb salvage: a single institution experience. *Int Orthop* 2002;26:197-202.
2. **Plötz W, Rechl H, Burgkart R, et al.** Limb salvage with tumor endoprostheses for malignant tumors of the knee. *Clin Orthop* 2002;405:207-15.
3. **Bickels J, Wittig JC, Kollender Y, et al.** Distal femur resection with endoprosthetic reconstruction: a long-term followup study. *Clin Orthop* 2002;400:225-35.
4. **Wunder JS, Leitch K, Griffin AM, Davis AM, Bell RS.** Comparison of two methods of reconstruction for primary malignant tumors at the knee: a sequential cohort study. *J Surg Oncol* 2001;77:89-99.
5. **Rödl RW, Ozaki T, Hoffmann C, et al.** Osteoarticular allograft in surgery for high-grade malignant tumours of bone. *J Bone Joint Surg [Br]* 2000;82-B:1006-10.
6. **Lane JM, Christ GH, Khan SN, Backus SI.** Rehabilitation for limb salvage patients: kinesiological parameters and psychological assessment. *Cancer* 2001;92:1013-19.
7. **Davis AM, Sennik S, Griffin AM, et al.** Predictors of functional outcomes following limb salvage surgery for lower-extremity soft tissue sarcoma. *J Surg Oncol* 2000;73:206-11.
8. **Refaat Y, Gunnoe J, Hornicek FJ, Mankin HJ.** Comparison of quality of life after amputation or limb salvage. *Clin Orthop* 2002;397:298-305.
9. **Kusuzaki K, Minami G, Takeshita H, et al.** Photodynamic inactivation with acridine orange on a multidrug-resistant mouse osteosarcoma cell line. *Jpn J Cancer Res* 2000;91:439-45.
10. **Kusuzaki K, Aomori K, Suginoshita T, et al.** Total tumor cell elimination with minimum damage to normal tissues in musculoskeletal sarcomas following photodynamic therapy with acridine orange. *Oncology* 2000;59:174-80.
11. **Hashiguchi S, Kusuzaki K, Murata H, et al.** Acridine orange excited by low-dose radiation has a strong cytocidal effect on mouse osteosarcoma. *Oncology* 2002;62:85-93.
12. **Kusuzaki K, Suginoshita T, Minami G, et al.** Fluorovisualization effect of acridine orange on mouse osteosarcoma. *Anticancer Res* 2000;20:3019-24.
13. **Kusuzaki K, Murata H, Takeshita H, et al.** Intracellular binding sites of acridine orange in living osteosarcoma cells. *Anticancer Res* 2000;20:971-5.
14. **Lewis MR, Goland PP.** In vivo staining and retardation of tumors in mice by acridine compounds. *Am J Med Sci* 1948;215:282-9.
15. **Korgaonkar KS, Sukhatankar JV.** Anti-tumour activity of the fluorescent dye, acridine orange, on Yoshida sarcoma (ascites). *Br J Cancer* 1963;17:471-3.
16. **Zdolsek JM, Olsson GM, Brunk UT.** Photooxidative damage to lysosomes of cultured macrophages by acridine orange. *Photochem Photobiol* 1990;51:67-76.
17. **Sastry KS, Gordon MP.** The photodynamic inactivation of tobacco mosaic virus and its ribonucleic acid by acridine orange. *Biochim Biophys Acta* 1966;129:32-41.
18. **Zampieri A, Greenberg J.** Mutagenesis by acridine orange and proflavine in Escherichia coli strain S. *Mutat Res* 1965;2:552-6.
19. **McCann J, Choi E, Yamasaki E, Ames BN.** Detection of carcinogens and mutagens in the Salmonella/microsome test: assay of 300 chemicals. *Proc Natl Acad Sci USA* 1975;72:5135-9.
20. **Giorgio A, Rambaldi M, Maccario P, Ambrosone L, Moles DA.** Detection of microorganisms in clinical specimens using slides prestained with acridine orange (AOS). *Microbiologica* 1989;12:97-100.
21. **Rickman LS, Oberst R, Long GW, et al.** Rapid diagnosis of malaria by acridine orange staining of centrifuged parasites. *Lancet* 1989;1:68-71.
22. **Kapuscinski J, Darzynkiewicz Z, Melamed MR.** Interactions of acridine orange with nucleic acids: properties of complexes of acridine orange with single stranded ribonucleic acid. *Biochem Pharmacol* 1983;32:3679-94.
23. **Amagasa J.** Mechanisms of photodynamic inactivation of acridine orange-sensitized transfer RNA: participation of singlet oxygen and base damage leading to inactivation. *J Radiat Res (Tokyo)* 1986;27:339-51.
24. **Zelenin AV.** Fluorescence microscopy of lysosomes and related structures in living cells. *Nature* 1966;212:425-6.
25. **Tomson SH, Emmett EA, Fox SH.** Photodestruction of mouse epithelial tumors after oral acridine orange and argon laser. *Cancer Res* 1974;34:3124-7.
26. **Tatsuta M, Yamamura H, Yamamoto R, et al.** Destruction of implanted gastric tumors in rats by acridine orange photoactivation with an argon laser. *Eur J Cancer Clin Oncol* 1984;20:543-52.
27. **Prosser E, Cox D, O'Kennedy R, Carroll K, van der Putten W.** Effects of coumarins, haematoporphyrins and acridine orange on the viability and growth of Landshütz ascites tumour cells, in the presence and absence of photoradiation. *Cancer Lett* 1990;52:71-7.
28. **Ishikawa S, Nemoto R, Kanoh S, Kobayashi K, Ishizaka S.** Photodynamic inactivation of bladder cancer cells (MGH-U1) sensitized with acridine orange and irradiated by argon laser. *Tohoku J Exp Med* 1984;144:265-71.
29. **Zdolsek JM.** Acridine orange-mediated photodamage to cultured cells. *Apmis* 1993;101:127-32.
30. **Van Duuren BL, Sivak A, Katz C, Melchionne S.** Tumorigenicity of acridine orange. *Br J Cancer* 1969;23:587-90.
31. **No authors listed.** Monographs on the evaluation of carcinogenic risks to humans. Vol. 16. 1978: 145. http://monographs.iarc.fr/ENG/Monographs/vol16/volume16.pdf (date last accessed 18 February 2010).
32. **Kato A.** Gastrofiberscopic diagnosis with acridine orange fluorescence. *Gastroenterol Endosc* 1970;12:351-62.
33. **Vrouenraets MB, Visser GW, Snow GB, van Dongen GA.** Basic principles, applications in oncology and improved selectivity of photodynamic therapy. *Anticancer Res* 2003;23:505-22.
34. **Sondak VK, Chang AE.** Clinical evaulation and treatment of soft tissue tumors. In: Weiss SW, Goldblum JR, eds. *Enzinger and Weiss's soft tissue tumors.* Fourth ed. St Louis: Mosby, 2001:28-32.
35. **Zagars GK, Ballo MT, Pisters PW, et al.** Prognostic factors for patients with localized soft-tissue sarcoma treated with conservation surgery and radiation therapy: an analysis of 1225 patients. *Cancer* 2003;97:2530-43.
36. **Duffaud F, Digue L, Mercier C, et al.** Recurrences following primary osteosarcoma in adolescents and adults previously treated with chemotherapy. *Eur J Cancer* 2003;39:2050-7.

Biochemical and Biophysical Research Communications 391 (2010) 1116–1121

Contents lists available at ScienceDirect

Biochemical and Biophysical Research Communications

journal homepage: www.elsevier.com/locate/ybbrc

Fibulin-3 negatively regulates chondrocyte differentiation

Toru Wakabayashi [a], Akihiko Matsumine [a,*], Shigeto Nakazora [a], Masahiro Hasegawa [a], Takahiro Iino [a], Hideki Ota [b], Hikaru Sonoda [b], Akihiro Sudo [a], Atsumasa Uchida [a]

[a] Department of Orthopaedic Surgery, Mie University Graduate School of Medicine, 2-174, Edobashi, Tsu-city, Mie 514-8507, Japan
[b] Shionogi Research Laboratories, Shionogi & Co., Ltd., 5-12-4, Sagisu, Fukushima-ku, Osaka 553-0002, Japan

ARTICLE INFO

Article history:
Received 3 December 2009
Available online 11 December 2009

Keywords:
Fibulin-3 (EFEMP1)
Extracellular matrix protein
Chondrogenesis
Chondrocyte differentiation
ATDC5

ABSTRACT

Fibulin-3 is a member of the fibulin family that has been newly recognized as extracellular matrix proteins. We assessed the effects of fibulin-3 overexpression on chondrocyte differentiation using the clonal murine cell line ATDC5. The ATDC5-FBLN3 stably expressing fibulin-3 protein was spindle-shaped cell compared to the ATDC5-mock with plump cell. The cell growth in the ATDC5-FBLN3 was accelerated in comparison to that in the ATDC5-mock. The ATDC5-FBLN3 was not stained by Alcian blue, nor was there any cartilage aggregate formed after the induction of chondrogenic differentiation. The expression of type II collagen, aggrecan, and type X collagen was completely suppressed in ATDC5-FBLN3 even after the induction of differentiation. The overexpression of fibulin-3 reduced the expression of *Sox5* and *Sox6*, while it maintained the expression of *Sox9*. These findings suggest that fibulin-3 may play an important role as a negative regulator of chondrocyte differentiation.

The complex multistep process of the development of skeletal elements through endochondral ossification is controlled by a variety of positive and negative regulators. Bone morphogenetic proteins (BMPs), transforming growth factor-β (TGF-β), fibroblast growth factors (FGFs), Indian hedgehog (Ihh), Wnts, and parathyroid hormone-related peptide (PTH-rP) positively regulate chondrocyte differentiation. At the transcription level, transcription factors such as Sox9, Sox5, Sox6, Runx2/Cbfa1, and DEC1 are critical for the induction and progression of chondrocyte differentiation [1–4]. In contrast, negative regulators such as epidermal growth factor (EGF), splicing factor 3b subunit 4 (SF3b4), retinoic acid receptor, aZfp60, c-fos, nuclear factor E2 p45-related factor 2 (Nrf 2), Notch, matrix metalloprotease-2 (MMP-2), and AP-2α suppress or delay chondrocyte differentiation [5–13]. The interplay of positive and negative regulators is essential to control chondrogenesis.

Fibulins are a newly recognized family of extracellular matrix glycoproteins with the distinctive features of a fibulin-type C-terminal domain preceded by tandem calcium-binding (cb) EGF-like modules. To date, the fibulin family consists of six members which are numerically named fibulin-1 through fibulin-6 [14,15]. Fibulin family proteins have unique and partially overlapping expression pattern. Tropoelastin is a common ligand for fibulins. Immunohistochemical analysis demonstrated that fibulins are localized in tissue rich in elastic fiber, such as lung, perichondrium, and blood vessels [14]. Fibulin-$5^{-/-}$ mice exhibited disrupted and disorganized elastic fibers throughout the body, suggesting that fibulin-5 may be involved in elastogenesis by tethering elastic fibers onto cell surface integrins [16,17]. Fibulin-$4^{-/-}$ mice exhibited almost complete loss of elastic fibers and perinatal lethality [18]. Fibulin-$3^{-/-}$ mice developed multiple large hernias and pelvic prolapse due to the loss of the integrity of elastic fibers in fascia connective tissue [19]. All these results indicate a distinct role of fibulin-3, -4, and -5 in elastic fiber formation. The resource of the fibulins considered to be primordial vascular smooth muscle cells, developing cartilage cells, endothelial cells of the artery [14,15,20–23]. Fibulin-3 was initially identified as a gene highly up-regulated in senescent and Werner syndrome fibroblasts [20]. Fibulin-3 is highly homologous to fibrillin which is the major causative gene of Marfan syndrome [15]. Genetic linkage and molecular analysis has associated a missense mutation (R345W) in fibulin-3 with heritable macular degenerative disorders, so-called Malattia Leventinese and Doyne honeycomb retinal dystrophy [21].

Fibulin-3 is highly expressed in cartilaginous tissue [14,22]. However, no direct evidence for the role of fibulin-3 underlying chondrocyte differentiation is available in the literature to date. The purpose of this study is to explore the function of fibulin-3 in chondrocyte differentiation.

Materials and methods

Construction of fibulin-3 expression vector and preparation of recombinant fibulin-3 protein. Using human EST clone: I.M.A.G.E. 6083389 (Invitrogen) as a template, a cDNA fragment corresponding

* Corresponding author. Fax: +81 59 231 5211.
E-mail address: matsumin@clin.medic.mie-u.ac.jp (A. Matsumine).

0006-291X/$ - see front matter © 2009 Elsevier Inc. All rights reserved.
doi:10.1016/j.bbrc.2009.12.034

to the entire open reading frame of fibulin-3 was amplified with the oligonucleotide primers 5′-AGCGGCCGCCACCATGTTGAAAGCCCTT TTCC-3′ and 5′-ATCTAGAAAATGAAAATGGC CCCAC-3′ by means of PCR, thus adding a NotI site at the 5′ end, XbaI site at the 3′ end and the termination codon substituted with a glycine codon. This fragment was cloned into NotI and XbaI sites in an expression vector p3xFLAG-CMV14 (Sigma–Aldrich) to generate p3xFLAG-FBLN3, in which human fibulin-3 cDNA was connected to a triple repeat of the FLAG tag sequence at the 3′ end. To generate recombinant fibulin-3 protein, p3xFLAG-FBLN3 was then cut off at the NotI and SphI sites and cloned into the NotI and SphI sites of vector pFastBac1 (Invitrogen, Tokyo, Japan). Using this plasmid, pFB-FBLN3, the human fibulin-3 protein connected to the FLAG tag at the C-terminus was expressed in a Bac-To-Bac Baculovirus expression system (Invitrogen, Tokyo, Japan) according to the manufacturer's instructions. The transfected Sf9 cells were cultivated as a source of recombinant baculovirus and the conditioned medium was substantially infected with freshly cultured Sf9 cells. After a 72-h incubation at 28 °C, transfected Sf9 cells were harvested and suspended in 50 mM Tris–HCl (pH 7.4), 0.15 M NaCl, 0.1 mM EDTA, 1 mM DTT, 0.1% NP-40 supplemented with one tablet per 50 ml of complete protease inhibitor cocktail (Roche Diagnostics, Tokyo, Japan), and then they were sonicated. After centrifugation, the soluble fraction was collected and applied to an anti-FLAG M2 affinity column (Sigma–Aldrich, Tokyo, Japan). Following washing with Tris-buffered saline (TBS) (pH 7.4), the fibulin-3-3xFLAG protein was eluted from the column with 100 mM glycine–HCl (pH 3.5) and neutralized with 1 M Tris–HCl (pH 8.0).

Cell culture. The mouse embryonal carcinoma-derived chondrogenic cell line ATDC5 was purchased from Cell Bank, RIKEN BioResource Center. The ATDC5 cells were cultured in the medium consisting of a 1:1 mixture of Dulbecco's modified Eagle's medium and Ham's F-12 medium containing 5% fetal bovine serum, 10 μg/ml human transferring (Roche Diagnostics), and 3×10^{-8} M sodium selenite (Sigma–Aldrich) at 37 °C in a humidified atmosphere of 5% CO_2 in air, as described [24]. For the induction of chondrogenesis, human recombinant insulin (Roche Diagnostics) at 10 μg/ml was added in the medium. To generate stable fibulin-3 expressing ATDC5 cells (ATDC5-FBLN3), p3xFLAG-FBLN3 was transfected to ATDC5 cells using Lipofectamine™ 2000 Reagent (Invitrogen), followed by culture in the selective medium containing 500 ng/ml G418 (Nacalai Tesque). To generate control clones of stable transfectants without fibulin-3 insert (ATDC5-mock), p3xFLAG vector was transfected to ATDC5 cells. For the analysis of cell growth of the ATDC5 cells, the cell lines were plated at a cell density of 1×10^4 cells in 12-well plates in the maintenance medium supplemented with human insulin. The cells were harvested after washing each plate three times with PBS. The cell number for each dish was counted with a cell counter.

Western blotting. We performed Western blotting using cell lysate and serum-free culture medium. The cell pellets were lysed in solubilization buffer. After centrifugation, the supernatant fluid was mixed to 6xSDS sample buffer and boiled for 5 min. Thereafter, the samples were separated in 10% SDS–PAGE, transferred onto poly vinylidene difluoride membranes (Millipore). After blocking the membrane with TBS-T containing 5% of non-fat dried milk, the membrane was immersed in the first antibody solution (a mouse monoclonal anti-β-actin antibody or anti-Flag M2 monoclonal antibody, Sigma–Aldrich) overnight at 4 °C. After washing with TBS-T, the membranes were incubated with HRP-conjugated anti-IgG antibody (GE Healthcare). The bands were visualized using the ECL plus Western blotting detection system (GE Healthcare) and detected by LAS-1000plus (Fuji film).

Alcian blue staining. On the predetermined day, the plates were washed two times with PBS, fixed with 95% methanol at −20 °C for 2 min, and stained with 0.1% Alcian blue (Muto Pure Chemicals) in 0.1 M HCl for 2 h. After rinsed three times with distilled water, the results were recorded with a digital camera. The dye was extracted with 6 M guanidine–HCl overnight, and the total optical density of extracted dye was measured using a spectrophotometer at 620 nm.

Total RNA extraction and quantitative real-time polymerase chain reaction. After washing each plate three times with cold PBS, the total RNA was extracted from the ATDC5 cells using ISOGEN (Nippon Gene), and 1.0 μg of RNA was reverse-transcribed with the First Strand cDNA Synthesis Kit (Roche Diagnostics). TaqMan Universal PCR Master Mix and TaqMan® Gene Expression Assays were used to analyze the genes including β-actin, Sox9, Sox5, Sox6, type II collagen, type X collagen, and aggrecan. Real-time quantitative PCR amplifications were performed on the ABI PRISM 7000 Sequence Detection System (Applied Biosystems). The C_t value of β-actin was used as an endogenous reference for normalization. Standard curves were generated using cDNA samples from ATDC5-mock on day 14 after induction of chondrogenic differentiation. The relative expression levels of each target gene were indicated by calculating the ratio for those from ATDC5-mock on day 14. Assays were performed in triplicate and repeated three times.

Northern blot analysis. The total RNA was extracted from the 1.0×10^7 ATDC5 cells using ISOGEN (Nippon Gene), Poly A^+ RNA was purified with an mRNA extraction kit (GE Healthcare), separated by agarose gel electrophoresis, and blotted onto a nylon (Hybond-N; GE Healthcare). Hybridization with β-actin cDNA was performed under the standard conditions described previously [20].

Statistics and analysis. The data were analyzed using the StatView statistical software program (version 5.0; SAS Institute). Statistical significance was set at a value of $p < 0.01$. Association with the variables was determined by *t*-test.

Results

Cell morphological and growth curve analysis

ATDC5 cells display a number of characteristics of committed chondroprogenitor cells and undergo insulin-induced chondrocyte differentiation, which resembles chondrocyte differentiation *in vivo* [24]. Thereafter, to investigate the effect of fibulin-3 on chondrocyte differentiation, we first isolated the subclones of the ATDC5 cell lines which stably express fibulin-3 protein (ATDC5-FBLN3). Among twelve isolated subclones, the three clones: clone#5, #10, and #12 expressed various amounts of fibulin-3 protein by a Western blotting (Fig. 1A). Therefore we employed these three clones for the following experiments as ATDC5-FBLN3. Meanwhile we generated three independent control clones of stable transfectants without the fibulin-3 insert (ATDC5-mock). It was found that the cell morphology of ATDC5-FBLN3 was drastically changed compared to the ATDC5-mock (Fig. 1B and C) and that ATDC5-FBLN3 was spindle-shaped although the proliferating ATDC5-mock cells were plump. Furthermore, we found that FBLN3 protein is indeed secreted into the culture medium at a concentration of 1 μg/ml to the medium (Fig. 1D), and that the cell proliferation in the ATDC5-FBLN3 was accelerated compared to that of ATDC5-mock (Fig. 1E).

The effect of fibulin-3 overexpression on production of proteoglycan and cartilage nodule formation

We next examined the effect of fibulin-3 overexpression on production of proteoglycan and cartilage nodule formation. As shown in Fig. 2A, the ATDC5-mock underwent progressive differentiation over the 28-day period in medium containing insulin, as evidenced by increased formation of cartilage aggregates and increased Alcian

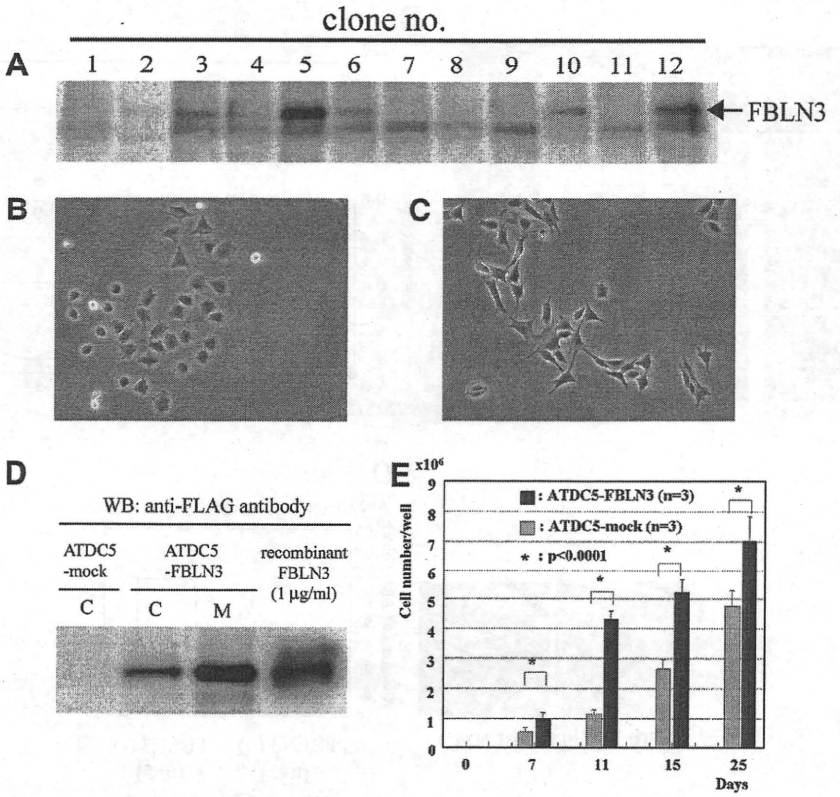

Fig. 1. Isolation of ATDC5-FBLN3. (A) ATDC5-FBLN3 which stably express FBLN3 was isolated. Among twelve isolated subclones, cell lysates from clone#5, #10, and #12 were revealed to contain the various amount of FBLN3 by a Western blot analysis. FBLN3: fibulin-3 protein. Microscopic findings showed that ATDC5-FBLN3 had spindle-shaped cytoplasm (C) although proliferating ATDC5-mock had plump cytoplasm (B). (D) Western blotting of cellular lysate and serum-free culture medium collected after 12-h incubation showed that fibulin-3 is indeed a secretory protein. C, cellular lysate; M, medium. To indicate the concentration of the fibulin-3 protein in the culture medium, recombinant fibulin-3 protein was applied at the concentration of 1 μg/ml into the far right lane. (E) Cell growth of ATDC5-mock and ATDC5-FBLN3. The cell proliferation in ATDC5-FBLN3 was accelerated in comparison to that of ATDC5-mock (gray box: ATDC5-mock, closed box: ATDC5-FBLN3). Independent three clones were examined, respectively. $^*p < 0.0001$.

blue staining. In contrast, the ATDC5-FBLN3 was not stained by Alcian blue, nor was there any cartilage aggregate formed. A quantitative determination of the extent of proteoglycan production showed that the overexpression of fibulin-3 resulted in the complete suppression during the induction of chondrogenesis (Fig. 2B). These results suggested that the overexpression of fibulin-3 protein suppressed cartilage aggregate formation and proteoglycan production despite induction.

The effect of the addition of exogenous recombinant fibulin-3 protein on ATDC5 differentiation

We presumed that the suppression of chondrogenic differentiation by fibulin-3 may cause a paracrine effect on the ATDC5 cells. Therefore we then generated recombinant fibulin-3 protein, and examined the effect of exogenous fibulin-3 protein on ATDC5 differentiation, adding this recombinant protein at a concentration of 1 μg/ml to the medium, which is the corresponding amount to secreted fibulin-3 protein in ATDC5-FBLN3 (Fig. 1D). The cartilage aggregates formation and production of proteoglycan in the ATDC5 cells were significantly suppressed (Fig. 2C and D). These results suggest that the suppression of chondrogenic differentiation by fibulin-3 did cause a paracrine effect on the ATDC5 cells.

The effect of fibulin-3 on chondrocyte differentiation at the molecular level

The effect of fibulin-3 on chondrocyte differentiation at the molecular level was further examined by quantitating the expression level of the chondrocyte marker gene: type II collagen, aggrecan, and type X collagen. Because the β-actin expression levels are not affected by either fibulin-3 or by chondrocyte differentiation (Fig. 3A), the β-actin was chosen as reference gene. As a result, the overexpression of fibulin-3 completely prevented the induction of type II collagen, while ATDC5-mock highly expressed type II collagen after induction of differentiation (Fig. 3B). Similar results were obtained with two other matrix genes: aggrecan and type X collagen genes (Fig. 3C and D). These results confirmed the overexpression of fibulin-3 indeed suppress chondrocyte differentiation.

The effect of fibulin-3 on expression of Sox9, Sox5, and Sox6 in ATDC5 cells

To understand the molecular mechanism of the inhibition of chondrocyte differentiation by fibulin-3, we examined the effect of fibulin-3 overexpression on the expression profiles of the Sox family of transcription factors such as Sox9, Sox5, and Sox6 which have been identified as key transcription factors required for early chondrogenesis [1,4,25]. Increased expression of Sox9 was observed in ATDC5-FBLN3 after stimulation with insulin, while the time in which the expression level of Sox9 reached to the peak level seemed to be one week later in ATDC5-FBLN3 than that in ATDC5-mock (Fig. 4A). The expression level of Sox5 in the ATDC5-mock increased at the beginning and early stage of chondrogenic differentiation (day 2), reached a peak expression level at day 4, and thereafter decreased. In contrast, the low expression level of Sox5 in the ATDC5-FBLN3 was stably observed before and after chondrogenic induction (Fig. 4B). The expression level of Sox6 in the ATDC5-mock was increased at the beginning and early stage of chondrogenic differentiation (day 4), and continued to increase

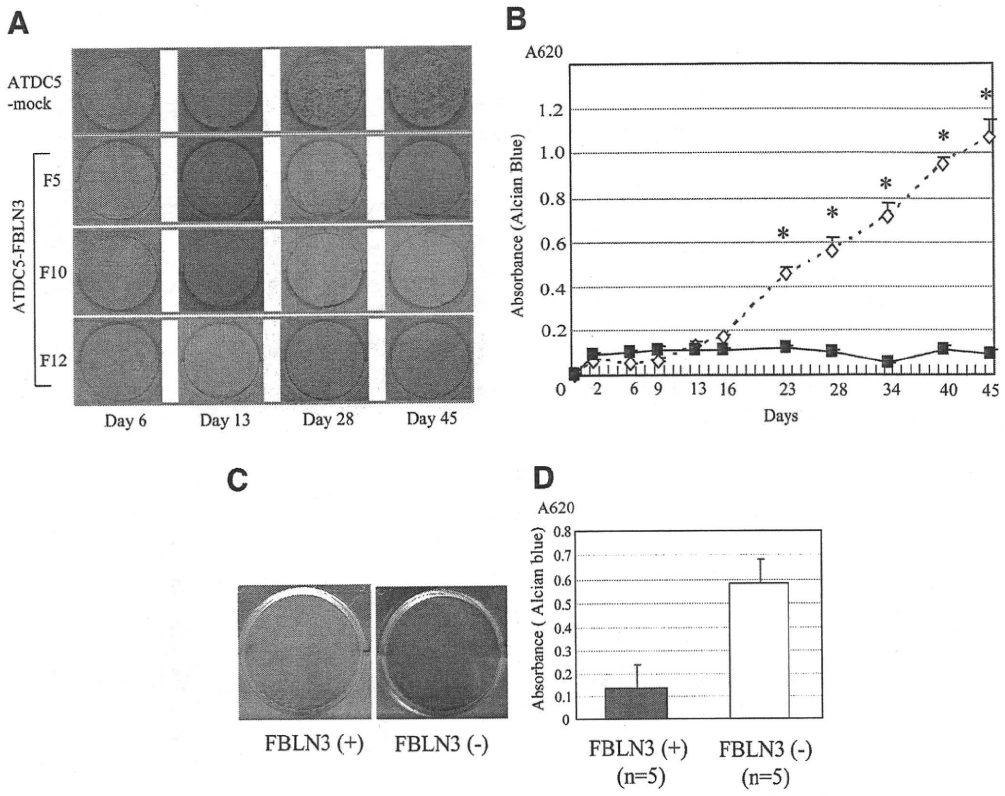

Fig. 2. The effect of fibulin-3 overexpression on cartilage nodule formation and production of proteoglycan. (A) ATDC5-mock underwent progressive differentiation in medium containing insulin, as evidenced by increased formation of cartilage aggregates and increased Alcian blue staining beginning at day 13. In contrast, ATDC5-FBLN3 was not stained by Alcian blue, nor were there any cartilage aggregates formed. (B) The quantitative determination of the extent of proteoglycan production showed the overexpression of fibulin-3 to result in the complete suppression in Alcian blue staining during the induction of chondrogenesis (open diamond: ATDC5-mock, closed square: ATDC5-FBLN3). Independent three clones were examined. $^{*}p < 0.0001$. (C, D) The effect of exogenous fibulin-3 protein on ATDC5 differentiation was examined by addition of the recombinant protein at a concentration of 1 μg/ml to the medium. The cartilage aggregates formation and production of proteoglycan were significantly suppressed at day 21 after induction of differentiation (C, D).

during the late stage of the differentiation. On the other hand, the expression levels of Sox6 in ATDC5-FBLN3 were completely suppressed during chondrogenic differentiation (Fig. 4C). These results demonstrated the overexpression of fibulin-3 reduce the expression of *Sox5* and *Sox6*, while maintaining the expression of *Sox9*.

Discussion

There have recently been several reports which describe the presence of fibulin-3 protein in cartilaginous tissue in the mouse embryo. Immunohistochemical analysis demonstrated fibulin-3 to be localized in the perichondrium in E15 mouse embryos [14]. An *in situ* analysis showed fibulin-3 to be found in the condensing mesenchymes, thus giving rise to bone and cartilage as well as in developing bone structures of the cranial and the axial skeleton [22]. During mouse embryogenesis, a very prominent expression of fibulin-2 was shown to be seen during the early stages of chondrogenesis in cartilaginous tissue [23]. These results suggest that fibulin-3 may thus play a possible role in organizing bone and cartilage development. However there have been no direct experimental studies which show the effect of fibulin-3 on chondrocyte differentiation.

In the present study, we demonstrated that fibulin-3 is a negative regulator of chondrocyte differentiation: the overexpression of fibulin-3 suppressed chondrocyte differentiation by inhibition of cartilage nodule formation, proteoglycan production, and matrix gene expression, and the overexpression of fibulin-3 selectively maintained the expression of *Sox9* but suppressed the expression of *Sox5* and *Sox6*. These results provide functional evidence showing that fibulin-3 is an important negative regulator in chondrocyte differentiation.

It was found that the cell morphology of ATDC5-FBLN3 was drastically changed. The ATDC5-FBLN3 cells were spindle-shape cells although proliferating ATDC5-mock cells were usually plump cells. The actin cytoskeleton is a primary determinant of cell shape. Recently, several interconnected transduction pathways and a number of signaling molecules which control actin cytoskeleton reorganization have been identified. In adherent cells, cell–matrix adhesions connect the extracellular matrix with the actin cytoskeleton and transmit forces in both directions. Interestingly, overexpression of the fibulin-3 in olfactory ensheathing cell (OEC) induced the more spindle-shape morphology with extremely long processes, compared to the control cultures of OEC. Furthermore, these effects of fibulin-3 were only present on matrigel, laminin, and collagen substrates but not PLL-coated cover slip [26]. These results suggest that possible interactions of fibulin-3 with these substrate components are influencing the cell morphology.

It was also found that the cell proliferation in ATDC5-FBLN3 was accelerated compared to that in ATDC5-mock. There are a few reports that indicate the effect of fibulin-3 on cell proliferation, but the findings remain controversial. The first evidence was that fibulin-3 is up-regulated in the senescent and Werner syndrome fibroblast, as well as in quiescent young fibroblasts. However paradoxically, a microinjection of the fibulin-3 gene into a Werner syndrome fibroblast consistently stimulated rather than inhibited DNA synthesis [20]. The effect of fibulin-3 on the cell proliferation may occur in a context specific manner and depends on the cell type.

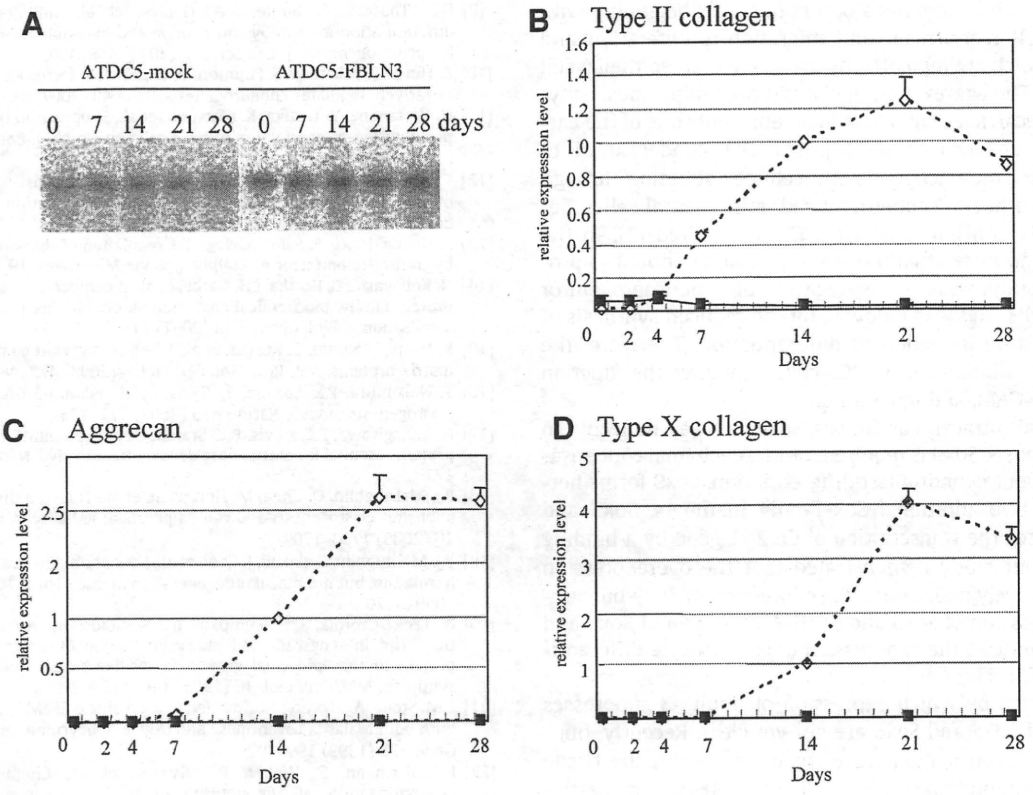

Fig. 3. The effect of fibulin-3 on chondrocyte differentiation at the molecular level. (A) The β-actin expression level detected with Northern blot analysis was not affected by either fibulin-3 or by chondrocyte differentiation. Thus, the β-actin was chosen as reference gene for the multiplex real-time PCR analysis. Overexpression of fibulin-3 completely prevented the induction of (B) type II collagen (C) aggrecan and (D) type X collagen genes, while ATDC5-mock highly expressed these three genes after induction of differentiation (open diamond: ATDC5-mock, closed square: ATDC5-FBLN3). Independent three clones were examined.

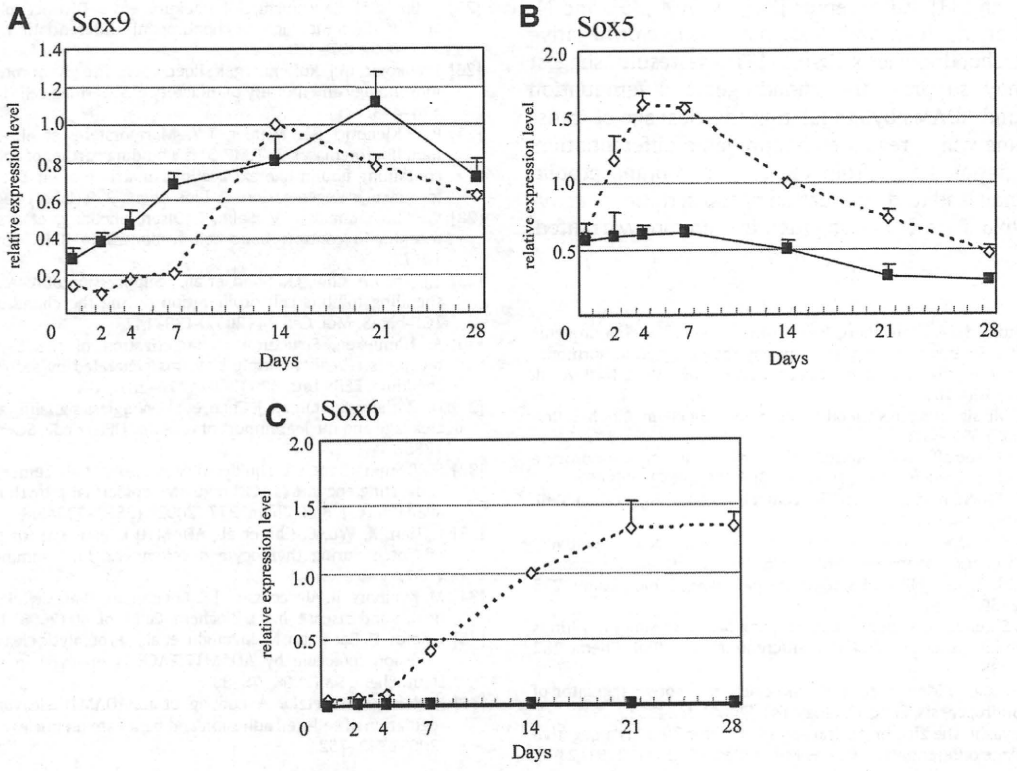

Fig. 4. The effect of the overexpression of fibulin-3 on expression of Sox9, Sox5, and Sox6 genes in ATDC5 cells. The overexpression of fibulin-3 maintained the expression of (A) Sox9, while reducing the expression of (B) Sox5 and (C) Sox6 after induction of differentiation (open diamond: ATDC5-mock, closed square: ATDC5-FBLN3). Independent three clones were examined.

The process of chondrogenesis occurs in stages beginning with mesenchymal cell recruitment and migration, proliferation and condensation, which are regulated by mesenchymal–epithelial cell interactions [4]. The aggregation of chondroprogenitor mesenchymal cells into precartilage condensations represents one of the earliest events in chondrogenesis [4]. For the condensation of chondroprogenitor mesenchymal cells, cell–cell adhesion through molecules such as neural cadherin (N-cadherin), neural cell adhesion molecule (N-CAM), and tenascin C are required [4]. In the present study, it appeared that the overexpression of fibulin-3 protein led to the suppression of aggregation of chondroprogenitor mesenchymal cells, and was followed by the reduced synthesis of proteoglycan despite induction of differentiation. Therefore, the overexpression of fibulin-3 in ATDC5 cells may alter the function of N-cadherin, N-CAM, and tenascin C.

Among several intracellular factors, Sox9 is a key molecule in early chondrogenesis. Sox9 is required for mesenchymal condensation and subsequent chondroblast differentiation. Sox9 forms heterodimers with two additional Sox family members, Sox5 and Sox6, and activates the transcription of Col2α1 gene by a binding enhancer [25]. Our study demonstrated that the overexpression of fibulin-3 selectively maintained the expression of Sox9 but suppressed the expression of Sox5 and Sox6. A reduction of Sox5 and Sox6 may contribute to the suppression of chondrocyte differentiation in ATDC5-FBLN3.

The mechanisms by which expression of fibulin-3 suppresses the expression of Sox5 and Sox6 are not yet clear. Recently, fibulin-3 protein has been demonstrated to interact with the tissue inhibitor of metalloproteinases-3 (TIMP-3). TIMP-3 is a matrix-bound inhibitor of matrix metalloproteinases (MMPs), a disintegrin and metalloproteinase-10 (ADAM-10), ADAM-17, a disintegrin and metalloproteinase with thrombospondin motif-4 (ADAMTS-4), and ADAMTS-5 [27]. Furthermore, ADAMs regulate the proteolytic cleavage of transmembrane receptor protein: BMP receptor [28], TGF-β receptor [29], FGF receptor [30], Wnt receptor [31], EGF receptor [32], Notch [33], IGF receptor [34], N-CAM [35], and N-cadherin [36], all of which are well-known as positive or negative regulators of the chondrogenesis [2–6,11]. These results suggest that fibulin-3 may suppress the chondrogenic differentiation through TIMP-3 and ADAMs by modulating the cleavage of transmembrane proteins which regulate chondrogenic differentiation. Reduced differentiation signal from the transmembrane protein due to fibulin-3 may lead to the reduction of transcriptional activity of Sox5 and Sox6. Further investigation is therefore warranted.

References

[1] W. Huang, U.I. Chung, H.M. Kronenberg, B. de Crombrugghe, The chondrogenic transcription factor Sox9 is a target of signaling by the parathyroid hormone-related peptide in the growth plate of endochondral bones, Proc. Natl. Acad. Sci. USA 98 (2001) 160–165.

[2] M. Wan, X. Cao, BMP signaling in skeletal development, Biochem. Biophys. Res. Commun. 18 (2005) 651–657.

[3] K.E. Yates, S. Shortkroff, R.G. Reish, Wnt influence on chondrocyte differentiation and cartilage function, DNA Cell Biol. 24 (2005) 446–457.

[4] M.B. Goldring, K. Tsuchimochi, K. Ijiri, The control of chondrogenesis, J. Cell. Biochem. 97 (2006) 33–44.

[5] Y.M. Yoon, C.D. Oh, D.Y. Kim, et al., Epidermal growth factor negatively regulates chondrogenesis of mesenchymal cells by modulating the protein kinase C-alpha, Erk-1, and p38 MAPK signaling pathways, J. Biol. Chem. 275 (2000) 12353–12359.

[6] H. Watanabe, M. Shionyu, T. Kimura, et al., Splicing factor 3b subunit 4 binds BMPR-IA and inhibits osteochondral cell differentiation, J. Biol. Chem. 282 (2007) 20728–20738.

[7] F. De Luca, J.A. Uyeda, V. Mericq, et al., Retinoic acid is a potent regulator of growth plate chondrogenesis, Endocrinology 141 (2000) 346–353.

[8] B. Ganss, H. Kobayashi, The zinc finger transcription factor Zfp60 is a negative regulator of cartilage differentiation, J. Bone Miner. Res. 17 (2002) 2151–2160.

[9] D.P. Thomas, A. Sunters, A. Gentry, et al., Inhibition of chondrocyte differentiation in vitro by constitutive and inducible overexpression of the c-fos proto-oncogene, J. Cell Sci. 113 (2000) 439–450.

[10] E. Hinoi, T. Takarada, S. Fujimori, et al., Nuclear factor E2 p45-related factor 2 negatively regulates chondrogenesis, Bone 40 (2007) 337–344.

[11] N. Watanabe, Y. Tezuka, K. Matsuno, et al., Suppression of differentiation and proliferation of early chondrogenic cells by Notch, J. Bone Miner. Metab. 21 (2003) 344–352.

[12] E.J. Jin, Y.A. Choi, E. Kyun Park, et al., MMP-2 functions as a negative regulator of chondrogenic cell condensation via down-regulation of the FAK-integrin beta1 interaction, Dev. Biol. 308 (2007) 474–484.

[13] Z. Huang, H. Xu, L. Sandell, Negative regulation of chondrocyte differentiation by transcription factor AP-2alpha, J. Bone Miner. Res. 19 (2004) 245–255.

[14] N. Kobayashi, G. Kostka, J.H. Garbe, et al., A comparative analysis of the fibulin protein family. Biochemical characterization, binding interactions, and tissue localization, J. Biol. Chem. 282 (2007) 11805–11816.

[15] R. Timpl, T. Sasaki, G. Kostka, et al., Fibulins: a versatile family of extracellular matrix proteins, Nat. Rev. Mol. Cell Biol. 4 (2003) 479–489.

[16] T. Nakamura, P.R. Lozano, Y. Ikeda, et al., Fibulin-5/DANCE is essential for elastogenesis in vivo, Nature 415 (2002) 171–175.

[17] H. Yanagisawa, E.C. Davis, B.C. Starcher, et al., Fibulin-5 is an elastin-binding protein essential for elastic fibre development in vivo, Nature 415 (2002) 168–171.

[18] P.J. McLaughlin, Q. Chen, M. Horiguchi, et al., Targeted disruption of fibulin-4 abolishes elastogenesis and causes perinatal lethality in mice, Mol. Cell. Biol. 26 (2006) 1700–1709.

[19] P.J. McLaughlin, B. Bakall, J. Choi, et al., Lack of fibulin-3 causes early aging and herniation, but not macular degeneration in mice, Hum. Mol. Genet. 16 (2007) 3059–3070.

[20] B. Lecka-Czernik, C.K. Lumpkin Jr., S. Goldstein, An overexpressed gene transcript in senescent and quiescent human fibroblasts encoding a novel protein in the epidermal growth factor-like repeat family stimulates DNA synthesis, Mol. Cell. Biol. 15 (1995) 120–128.

[21] E.M. Stone, A.J. Lotery, F.L. Munier, et al., A single EFEMP1 mutation associated with both Malattia Leventinese and Doyne honeycomb retinal dystrophy, Nat. Genet. 22 (1999) 199–202.

[22] J. Ehlermann, S. Weber, P. Pfisterer, et al., Cloning, expression and characterization of the murine Efemp1, a gene mutated in Doyne-Honeycomb retinal dystrophy, Gene Expr. Patterns 3 (2003) 441–447.

[23] H.Y. Zhang, R. Timpl, T. Sasaki, et al., Fibulin-1 and fibulin-2 expression during organogenesis in the developing mouse embryo, Dev. Dyn. 205 (1996) 348–364.

[24] C. Shukunami, C. Shigeno, T. Atsumi, et al., Chondrogenic differentiation of clonal mouse embryonic cell line ATDC5 in vitro: differentiation-dependent gene expression of parathyroid hormone (PTH)/PTH-related peptide receptor, J. Cell Biol. 133 (1996) 457–468.

[25] T. Ikeda, H. Kawaguchi, S. Kamekura, et al., Distinct roles of Sox5, Sox6, and Sox9 in different stages of chondrogenic differentiation, J. Bone Miner. Metab. 23 (2005) 337–340.

[26] J. Vukovic, M.J. Ruitenberg, K. Roet, et al., The glycoprotein fibulin-3 regulates morphology and motility of olfactory ensheathing cells in vitro, Glia 57 (2009) 424–443.

[27] P.A. Klenotic, F.L. Munier, L.Y. Marmorstein, et al., ; Tissue inhibitor of metalloproteinases-3 (TIMP-3) is a binding partner of epithelial growth factor-containing fibulin-like extracellular matrix protein 1 (EFEMP1). Implications for macular degenerations, J. Biol. Chem. 279 (2004) 30469–30473.

[28] W. Singhatanadgit, V. Salih, I. Olsen, Shedding of a soluble form of BMP receptor-IB controls bone cell responses to BMP, Bone 39 (2006) 1008–1017.

[29] E.J. Jin, Y.A. Choi, J.K. Sonn, et al., ; Suppression of ADAM 10-induced Delta-1 shedding inhibits cell proliferation during the chondro-inhibitory action of TGF-beta3, Mol. Cell 24 (2007) 139–147.

[30] A. Hanneken, Structural characterization of the circulating soluble FGF receptors reveals multiple isoforms generated by secretion and ectodomain shedding, FEBS Lett. 489 (2001) 176–181.

[31] D. Mathew, B. Ataman, J. Chen, et al., Wingless signaling at synapses is through cleavage and nuclear import of receptor DFrizzled2, Science 310 (2005) 1284–1285.

[32] S.W. Sunnarborg, C.L. Hinkle, M. Stevenson, et al., Tumor necrosis factor-alpha converting enzyme (TACE) regulates epidermal growth factor receptor ligand availability, J. Biol. Chem. 277 (2002) 12838–12845.

[33] L. Tian, X. Wu, C. Chi, et al., ADAM10 is essential for proteolytic activation of Notch during thymocyte development, Int. Immunol. 20 (2008) 1181–1187.

[34] M. Kveiborg, R. Albrechtsen, J.R. Couchman, et al., Cellular roles of ADAM12 in health and disease, Int. J. Biochem. Cell Biol. 40 (2008) 1685–1702.

[35] I. Kalus, U. Bormann, M. Mzoughi, et al., ; Proteolytic cleavage of the neural cell adhesion molecule by ADAM17/TACE is involved in neurite outgrowth, J. Neurochem. 98 (2006) 78–88.

[36] K. Reiss, T. Maretzky, A. Ludwig, et al., ADAM10 cleavage of N-cadherin and regulation of cell–cell adhesion and beta-catenin nuclear signaling, EMBO J. 24 (2005) 742–752.

Journal of Orthopaedic Surgery 2010;18(3):346-51

Percutaneous vertebroplasty for osteoporotic compression fractures using calcium phosphate cement

Shigeo Ishiguro,[1] Yuichi Kasai,[2] Akihiro Sudo,[2] Koji Iida,[1] Atsumasa Uchida[2]
[1] Department of Orthopaedic Surgery, Oyamada Memorial Spa Hospital, Yokkaichi, Mie, Japan
[2] Department of Orthopaedic Surgery, Mie University Graduate School of Medicine, Mie, Japan

ABSTRACT

Purpose. To compare percutaneous transpedicular vertebroplasty using calcium phosphate cement (CPC) versus conservative treatment for osteoporotic vertebral fractures.

Methods. Eight men and 28 women aged 61 to 99 (mean, 80) years with osteoporotic vertebral fractures underwent percutaneous transpedicular vertebroplasty using CPC. During the same period, 6 men and 32 women aged 53 to 93 (mean, 77) years underwent conservative treatment. The indication for vertebroplasty was a painful unstable fracture, with mobility of the vertebral body shown on flexion and extension lateral radiographs. Fractures without mobility despite deformity were treated conservatively.

Results. In the vertebroplasty group, all patients benefited from reduced back pain immediately after surgery, and pain relief was maintained at the latest follow-up. However, correction loss continued until one month after the operation. The mean visual analogue score for pain decreased significantly from preoperation to one day after surgery (9.3 vs. 6.2, p=0.02), and further decreased to 2.8 (p=0.04) on day 3 or 4 when ambulation began, and to 1.5 at the one-month follow-up and 1.4 at the final follow-up (mean, 14 months). The mean duration of analgesic treatment was significantly shorter in the vertebroplasty than conservatively treated group (10.2 vs. 63.5 days). All patients in the vertebroplasty group achieved bone union, with no adjacent vertebral fractures. However, in patients having conservative treatment, there were 2 adjacent vertebral fractures and 4 pseudarthroses, and the collapse continued for several months.

Conclusion. Percutaneous transpedicular vertebroplasty using CPC achieves immediate pain relief and reduces the risk of vertebral body collapse and pseudarthrosis among elderly patients with osteoporotic vertebral compression fractures.

Key word: *bone cements; fractures, compression; polymethyl methacrylate; vertebroplasty*

Address correspondence and reprint requests to: Dr Shigeo Ishiguro, Department of Orthopaedic Surgery, Oyamada Memorial Spa Hospital, Yamada-cho, Yokkaichi City, Mie Prefecture, Japan. E-mail: stoneblack1496@syutaikai.jp

INTRODUCTION

Augmentation of the vertebral body, also known as vertebroplasty, by percutaneous polymethylmethacrylate (PMMA) injection is useful for elderly patients with osteoporotic compression fractures.[1-5] Several new biological bone cement substitutes have been developed and proved to be useful.[6-9] Calcium phosphate cement (CPC) can be prepared as an injectable paste.[10] The compressive strength of CPC is lower than that of PMMA (80 vs. 99 MPa),[7,11,12] but both were greater than in osteoporotic vertebral bodies.

MATERIALS AND METHODS

This study was approved by the ethics committee and the institutional review board of our hospitals. Between April 2003 and March 2006, 8 men and 28 women aged 61 to 99 (mean, 80) years with unstable (mobility of the vertebral body on flexion and extension lateral radiographs) thoracic or lumbar osteoporotic vertebral fractures underwent percutaneous transpedicular vertebroplasty using CPC. All patients complained of back/low back pain and difficulty in sitting and standing, but none had neurological deficits. Three of 36 patients had 3 vacuum clefts. The injury mechanism in 24 patients was associated with trivial trauma (falling on the buttocks or stooping); 6 denied any trauma and were considered to have had spontaneous osteoporotic fractures; and the remaining 6 were due to unknown aetiology. During the same period, 6 men and 32 women aged 53 to 93 (mean, 77) years with stable osteoporotic vertebral fractures underwent conservative treatment. Haematomas, soft tissues or vacuum clefts were identified, and tumours or infections were ruled out using magnetic resonance imaging.

Bone mineral density of patients in both groups was compared (Table). The kyphosis index of the vertebral body was measured on flexion-extension lateral radiographs, expressed as the percentage of vertebral body height at the anterior region compared with its height at the posterior region. The mobility ratio was defined as the difference between the kyphosis index in extension and flexion. The deformity angle was also measured on flexion-extension lateral radiographs, expressed as the angle formed by the upper and lower ends of the anterior vertebral body.

The pre- and post-operative kyphosis index and the deformity angle of the vertebral body were compared using the paired *t*-test. A p value of <0.05 was considered statistically significant. Bone union was determined by stability on flexion-extension lateral radiographs, persistence of the kyphosis index and deformity angle on the serial radiographs, and the presence of callus bridging on computed tomography.

Surgical techniques

The patient was placed in the prone position under general anaesthesia. A longitudinal incision was made bilaterally over the pedicles, and 2 guide pins were inserted percutaneously and transpedicularly. Both sides of the pedicle were fenestrated using a cannulated drilling system and a dilation technique. Prods (made from 3- or 4-mm Steinmann pins) were introduced into the vertebral body for reduction and spreading of cavity.

A 1-ml syringe was inserted into the cavity along the 3-mm Steinmann pin. After removal of the Steinmann pin, the syringe was used as a port. The vertebral body was irrigated by saline poured into one entrance pedicle and flowed out of the other (Fig. 1). In cases where the inflow and outflow seemed unequal, leakage was checked during routine intravertebral injection of the contrast medium. In 2 cases suspected of leakage, the contrast medium was injected with the outflow blocked by the finger.

Table
Comparison of patients undergoing vertebroplasty versus conservative treatment

Parameter	Vertebroplasty (n=36)	Conservative treatment (n=38)
Mean±SD bone mineral density (g/cm^2)	0.438±0.030	0.407±0.023
Fracture site (no. of patients)		
T8	0	1
T9	1	1
T10	1	1
T11	2	1
T12	8	6
L1	11	14
L2	6	6
L3	4	3
L4	1	4
L5	2	1
No. of adjacent vertebral fractures	0	2
No. of pseudoarthrosis*	0	4

* p=0.02

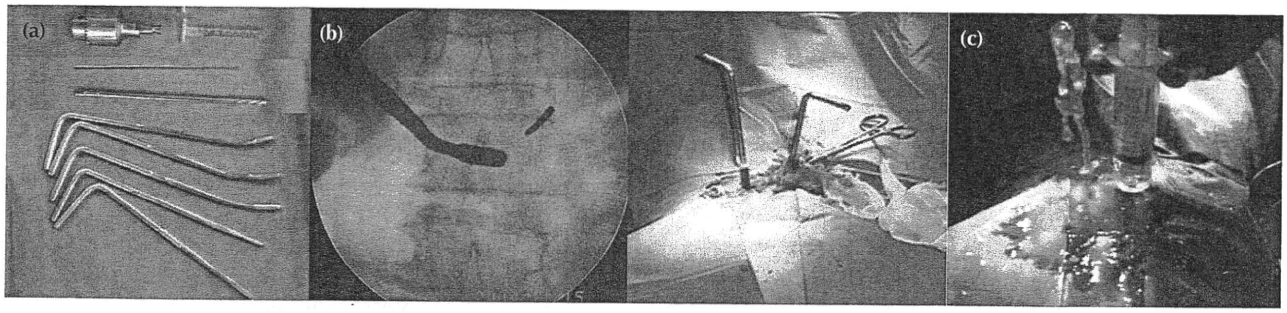

Figure 1 (a) The guide pins, 1-ml syringe, 2.5-mm cannulated drill, and reduction and spreading prods are shown. (b) Reduction and spreading prods are inserted into the vertebral body through the left pedicle. (c) Saline is poured into one entrance pedicle and flows out of another.

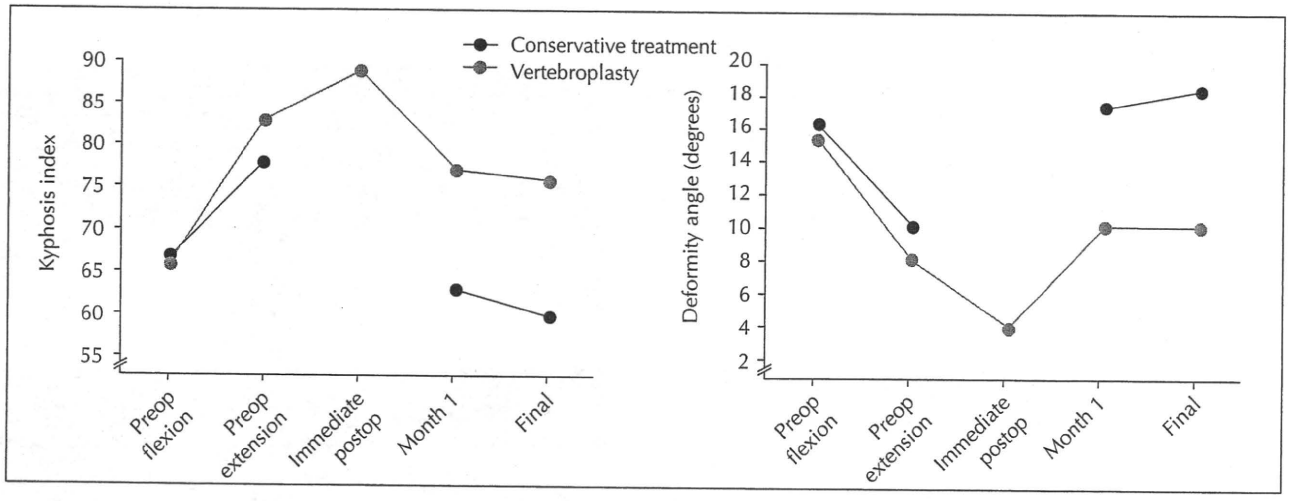

Figure 2 Improvement of the kyphosis index and deformity angle on flexion are significantly better after vertebroplasty than conservative treatment.

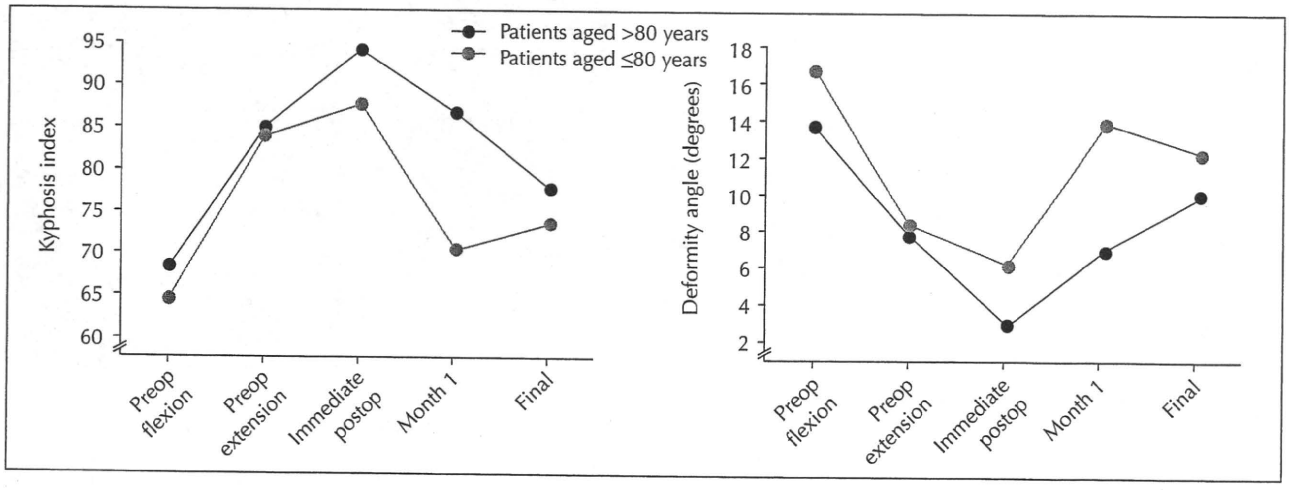

Figure 3 Among patients undergoing vertebroplasty, patients aged >80 years have a correction loss after one month, compared to little correction loss in patients aged ≤80 years, based on the kyphosis index.

CPC with a powder/liquid ratio of 2.8 to 3.3 was prepared and kneaded at room temperature for one to 3 minutes. The size of the cavity was usually <3 ml, but 6 ml of CPC was used as filler to prevent its dilution. In cases of confirmed leakage of contrast medium into the spinal canal, CPC was carefully injected under image intensifier guidance. CPC was introduced from the anterior to the posterior wall. The moment the CPC reached the posterior wall, injection was stopped. With the aid of fluoroscopic guidance, in some cases, injection was stopped when surplus CPC–stained blood entered the syringe in the opposite pedicle. Debris around the portal was removed, and the skin wounds closed.

RESULTS

The mean interval from injury to surgery was 11 (range, 1–22) days. The mean operating time was 30 (range 20–40) minutes. Intra-operative blood loss was insignificant. Ambulation was allowed after 3 or 4 days. In the vertebroplasty group, all patients showed reduced back pain immediately after surgery, and pain relief was maintained at the latest follow-up. The mean visual analogue score[13] for pain decreased significantly from preoperation to one day after surgery (9.3 [range, 9–10] vs. 6.2 [range, 5–8], p=0.02, paired-*t* test) and further decreased to 2.8 (range, 1–5) [p=0.04, paired-*t* test] on day 3 or 4 when ambulation began, and to 1.5 at the one-month follow-up and 1.4 at the final follow-up (mean, 14 months; range, 12–27 months). The mean duration of analgesic treatment was significantly lower in the vertebroplasty group (10.2 vs. 63.5 days, p=0.003).

Kyphosis index and deformity angle of vertebral body

In the vertebroplasty group, the mean preoperative kyphosis index and deformity angle on flexion were 66% and 15°, respectively. The values improved to 89% and 4° immediately after surgery (p<0.0001 in both, paired-*t* test, Fig. 2), but at the one-month follow-up there was a correction loss and the values regressed significantly to 77% and 10°, respectively (p=0.004 and 0.0004, respectively). The values were unchanged at the one-year follow-up and compared favourably than those measured preoperatively (p=0.0003 and p<0.0001, respectively, paired-*t* test, Fig. 2), with the mean improvement of 9% and 4°, respectively. Vertebral body collapse and pseudarthrosis appeared to have been prevented. Therefore, no adjacent vertebral fractures were encountered (compared to 2 in those underwent conservative treatment) [Table].

At the one-month follow-up, patients in the vertebroplasty group retained a significantly better kyphosis index and deformity angle than those treated conservatively (p<0.0001 in both, unpaired *t* test). All cases in the vertebroplasty group achieved bone union, whereas among conservatively treated patients 4 developed pseudarthroses (p=0.02, Chi-squared test and analysis-variance techniques, Table).

Among the vertebroplasty group, 2 men and 16 women aged >80 (mean, 86) years had a correction loss after one month, compared to the remaining 6 men and 12 women aged ≤80 (mean, 73) years with little correction loss, based on the kyphosis index

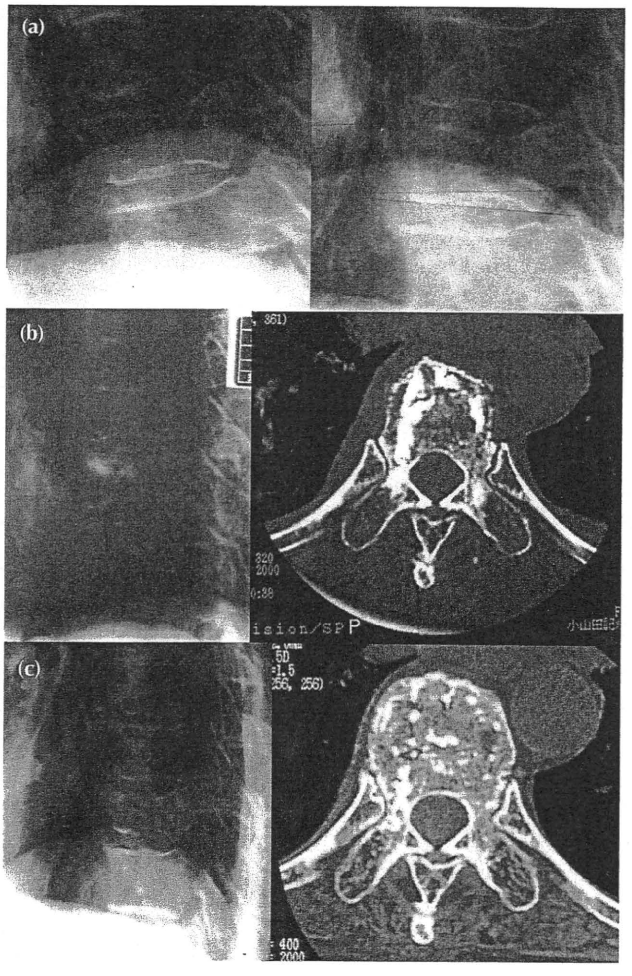

Figure 4 **(a)** Preoperative flexion and extension radiographs of an 87-year-old man showing deformity angles of 8° and 5°, and kyphosis indices of 81% and 92%, respectively. **(b)** Immediate postoperation and **(c)** one-year follow-up showing a correction loss and gradual absorption of calcium phosphate cement and replacement by new bone.

(p=0.0168, unpaired *t* test, Fig. 3).

Complications

No patient had temporary respiratory insufficiency during vertebroplasty. Three patients had a small amount of CPC leaked into the paravertebral muscle, but experienced no symptoms.

DISCUSSION

Adjacent vertebral compression fractures have been reported in PMMA balloon kyphoplasties[14–16]; some authors advocate the use of CPCs to decrease the incidence of such fractures.[14]

In a study of *in situ* vertebroplasty using CPC, advanced patient age, female gender, high bone mineral density, a short interval from injury to surgery, and injection via the unipedicular route may increase the incidence of CPC leakage.[17] In our series, the leakage rate was small (compared to 35% in that study), because our augmentation technique made space inside the vertebral cavity so as not to increase the pressure on filling the CPC bilaterally. When leakage was expected, CPC was injected very slowly in small amounts over a wider space under image intensifier guidance.

Postoperative correction loss after Biopex R-assisted *in situ* vertebroplasty has been reported.[7,18] Although our patients were more senile and severely osteoporotic, height restoration using reduction and spreading prods was better than in those series of *in situ* vertebroplasty with neither reduction nor spacing the fracture site (Fig. 4).

The presence of a haematoma and the low powder/liquid ratio of CPC decrease its compressive strength,[19] and may compromise the success rate. Therefore, new devices and techniques for percutaneous reduction and spacing of the vertebral body were used. The injection of CPC did not induce pressure elevation, which can cause pulmonary embolism and CPC leakage into the spinal canal. Moreover, the technique of using 1-ml syringes in the pedicles prevented CPC leakage into the spinal canal through pedicle fractures (if they existed).

In one study, cement leakage occurred in 41% and 9% of vertebrae treated with vertebroplasty and kyphoplasty, respectively.[15] In our series, CPC leakage was 8% and comparable to balloon kyphoplasty. Our method is more cost-effective than balloon kyphoplasty.

REFERENCES

1. Bostrom MP, Lane JM. Future directions. Augmentation of osteoporotic vertebral bodies. Spine (Phila Pa 1976) 1997;22(24 Suppl):S38–42.
2. Cotten A, Dewatre F, Cortet B, Assaker R, Leblond D, Duquesnoy B, et al. Percutaneous vertebroplasty for osteolytic metastases and myeloma: effects of the percentage of lesion filling and the leakage of methyl methacrylate at clinical follow-up. Radiology 1996;200:525–30.
3. Deramond H, Depriester C, Galibert P, Le Gars D. Percutaneous vertebroplasty with polymethylmethacrylate. Technique, indications, and results. Radiol Clin North Am 1998;36:533–46.
4. Gangi A, Kastler BA, Dietemann JL. Percutaneous vertebroplasty guided by a combination of CT and fluoroscopy. AJNR Am J Neuroradiol 1994;15:83–6.
5. Konno S, Olmarker K, Byrod G, Nordborg C, Stromqvist B, Rydevik B. The European Spine Society AcroMed Prize 1994. Acute thermal nerve root injury. Eur Spine J 1994;3:299–302.
6. Constantz BR, Ison IC, Fulmer MT, Poser RD, Smith ST, VanWagoner M, et al. Skeletal repair by in situ formation of the mineral phase of bone. Science 1995;267:1796–9.
7. Nakano M, Hirano N, Matsuura K, Watanabe H, Kitagawa H, Ishihara H, et al. Percutaneous transpedicular vertebroplasty with calcium phosphate cement in the treatment of osteoporotic vertebral compression and burst fractures. J Neurosurg 2002;97(3 Suppl):S287–93.
8. Bai B, Jazrawi LM, Kummer FJ, Spivak JM. The use of an injectable, biodegradable calcium phosphate bone substitute for the prophylactic augmentation of osteoporotic vertebrae and the management of vertebral compression fractures. Spine (Phila Pa 1976) 1999;24:1521–6.
9. Oner FC, Dhert WJ, Verlaan JJ. Less invasive anterior column reconstruction in thoracolumbar fractures. Injury 2005;36(Suppl 2):B82–9.
10. Ikeuchi M, Yamamoto H, Shibata T, Otani M. Mechanical augmentation of the vertebral body by calcium phosphate cement injection. J Orthop Sci 2001;6:39–45.
11. Ledlie JT, Renfro M. Balloon kyphoplasty: one-year outcomes in vertebral body height restoration, chronic pain, and activity levels. J Neurosurg 2003;98(1 Suppl):S36–42.
12. Almirall A, Larrecq G, Delgado JA, Martinez S, Planell JA, Ginebra MP. Fabrication of low temperature macroporous hydroxyapatite scaffolds by foaming and hydrolysis of an alpha-TCP paste. Biomaterials 2004;25:3671–80.
13. Huskisson EC. Measurement of pain. Lancet 1974;2:1127–31.

14. Heini PF, Berlemann U. Bone substitutes in vertebroplasty. Eur Spine J 2001;10(Suppl 2):S205–13.
15. Hulme PA, Krebs J, Ferguson SJ, Berlemann U. Vertebroplasty and kyphoplasty: a systematic review of 69 clinical studies. Spine (Phila Pa 1976) 2006;31:1983–2001.
16. Lee WS, Sung KH, Jeong HT, Sung YS, Hyun YI, Choi JY, et al. Risk factors of developing new symptomatic vertebral compression fractures after percutaneous vertebroplasty in osteoporotic patients. Eur Spine J 2006;15:1777–83.
17. Nakano M, Hirano N, Ishihara H, Kawaguchi Y, Matsuura K. Calcium phosphate cement leakage after percutaneous vertebroplasty for osteoporotic vertebral fractures: risk factor analysis for cement leakage. J Neurosurg Spine 2005;2:27–33.
18. Nakano M, Hirano N, Ishihara H, Kawaguchi Y, Watanabe H, Matsuura K. Calcium phosphate cement-based vertebroplasty compared with conservative treatment for osteoporotic compression fractures: a matched case-control study. J Neurosurg Spine 2006;4:110–7.
19. Garfin SR, Yuan HA, Reiley MA. New technologies in spine: kyphoplasty and vertebroplasty for the treatment of painful osteoporotic compression fractures. Spine (Phila Pa 1976) 2001;26:1511–5.

J Orthop Sci (2010) 15:666–673
DOI 10.1007/s00776-010-1513-x

JOURNAL OF
ORTHOPAEDIC SCIENCE

Original article

Distribution and role of tenascin-C in human osteoarthritic cartilage

YUTAKA NAKOSHI[1], MASAHIRO HASEGAWA[1], KOJI AKEDA[1], TAKAHIRO IINO[1], AKIHIRO SUDO[1], TOSHIMICHI YOSHIDA[2], and ATSUMASA UCHIDA[1]

[1]Department of Orthopedic Surgery, Mie University Graduate School of Medicine, 2-174 Edobashi, Tsu City, Mie 514-8507, Japan
[2]Department of Pathology and Matrix Biology, Mie University Graduate School of Medicine, Tsu City, Mie, Japan

Abstract

Background. Tenascin-C (TN-C) is expressed in the cartilage of osteoarthritis (OA). We examined whether TN-C was involved in cartilage repair of the diseased joints. Human articular cartilage samples were obtained from patients with OA and those with normal joints.

Methods. Immunohistochemistry testing of TN-C, chondroitin sulfate (CS), and proliferating cell nuclear antigen (PCNA) was performed. Chondrocytes were isolated from human cartilage and cultured. After treatment with TN-C, chondrocyte proliferation s was analyzed by bromodeoxyuridine (BrdU) incorporation assay using an enzyme-linked immunosorbent assay kit. Glycosaminoglycan content was determined by dimethylmethylene blue (DMMB) assay. The mRNA expression of aggrecan was also analyzed, by quantitative real-time polymerase chain reaction (PCR).

Results. In osteoarthritic cartilage, increased TN-C staining was observed with the degeneration of articular cartilage in comparison with normal cartilage. TN-C staining was shown in the cartilage surface overlying CS-positive areas. In addition, the expression of PCNA in the positive areas for TN-C was significantly higher than that in the negative areas. Treatment of human articular chondrocytes with 10 μg/ml TN-C accelerated chondrocyte proliferation, increased the proteoglycan amount in culture, and increased the expression of aggrecan mRNA.

Conclusions. Our findings indicate that the distribution of TN-C is related to CS production and chondrocyte proliferation in osteoarthritic cartilage and that TN-C has effects on DNA synthesis, proteoglycan content, and aggrecan mRNA expression in vitro. TN-C may be responsible for repair in human osteoarthritic cartilage.

Offprint requests to: M. Hasegawa
Received: November 10, 2009 / Accepted: May 31, 2010

Introduction

Osteoarthritis (OA) is the most prevalent musculoskeletal disease and is characterized by the degradation of cartilage.[1] Recent studies have demonstrated that some growth factors, including basic fibroblast growth factor (bFGF), transforming growth factor-β (TGF-β), insulin-like growth factor-I, and bone morphogenetic protein, are upregulated in OA cartilage and that they could stimulate chondrocyte proliferation and/or production of the cartilage matrix.[2] These molecules may promote cartilage repair in OA and suppress the disease progression.

Tenascin-C (TN-C) is an extracellular matrix glycoprotein composed of six similar subunits linked in their amino-terminal domain by disulfide bonds.[3] TN-C is predominantly expressed during embryogenesis.[4] Although TN-C expression is restricted in normal adult tissues, it reappears in association with wound healing, inflammatory processes, or neoplasia in a number of tissues.[5] In the neoplastic lesions, TN-C promotes the proliferation and migration of epithelial and mesenchymal cells.[6,7] TN-C has been found to be a constituent of developing articular cartilage, but the expression of TN-C was markedly decreased in adult normal articular cartilage.[8,9] In diseased joints, including those with OA, TN-C was highly re-expressed in human cartilage.[10] A previous study has shown that the TN-C concentration was elevated in synovial fluid obtained with cartilage lesions of the knee joint.[11] We have also demonstrated that levels of TN-C in joint fluids seem to parallel the radiographic progression of OA.[12] However, it is still unclear whether the TN-C expressed in the diseased joints prevents the cartilage damage or accelerates it.

In this study, we hypothesized that TN-C may contribute to articular cartilage repair in OA. Immunohistochemically, we observed the distribution of TN-C expressed in OA cartilage and examined its correlation

with the proliferation of chondrocytes, using proliferating cell nuclear antigen (PCNA) and the deposition of sulfated glucosaminoglycans in the joint cartilage. Furthermore, the effects of TN-C on chondrocyte proliferation, glycosaminoglycan content, and the mRNA level of aggrecan were investigated in vitro. We investigated whether TN-C was involved in cartilage repair of diseased joints.

Materials and methods

Cartilage specimens

Human OA cartilage specimens were obtained from the femoral condyles of 36 patients, aged 63–87 years (average, 72.9 years) who were undergoing total knee joint replacement for the treatment of OA. Non-OA cartilage specimens were obtained from the femoral condyles of 4 patients aged 19–33 years (average, 24.4 years) with no history of joint disease and no evidence of macroscopic articular degeneration at the time of amputation for tumor resection. All patients gave their informed consent and this study was approved by the local ethics committee. The specimens were immediately fixed in 4% paraformaldehyde in 0.1% phosphate-buffered saline (PBS; pH 7.4) at room temperature (RT) overnight, decalcified in treated K-CX (Falma, Tokyo, Japan), and embedded in paraffin. The sections were cut at 5-μm thickness and placed on Silane-coated glass-slides (Matsunami, Osaka, Japan). Serial sections were stained with safranin O, and we assessed cartilage destruction in each area using Mankin's scoring system, a 14-point scoring system for histological findings.[13] Based on the sum of the scores, each section was ranked as one of four histological grades: normal, 0–2; mild, 3–6; moderate, 7–10; and severe, 11–14.

Chondrocyte isolation and culture

Chondrocytes were isolated from human articular cartilage during knee replacements for advanced OA under sterile conditions. Cartilage fragments, damaged by fibrillation resulting from OA change, were removed from the femoral condyles of knee joints with a sharp curette. The cartilage fragments were incubated in 0.8% Pronase solution (Calbiochem, Darmstadt, Germany) and dissolved in Dulbecco's modified Eagle's medium/Ham F12 (DMEM/F12) (GIBCO, Grand Island, NY, USA) for 30 min at 37°C with continuous agitation in an atmosphere of 5% CO_2. After washing with DMEM/F12, the cartilage pieces were incubated with 0.4% collagenase (Roche Diagnostics, Penzberg, Germany) in DMEM/F12 for 90 min at 37°C with orbital mixing. The cell suspension was filtered using a 70-μm pore size nylon filter (BD Biosciences, Bedford, MA, USA) to remove the tissue debris. The filtrate was centrifuged for 5 min at 1200 rpm. The cells were washed with DMEM/F12 containing 10% fetal bovine serum (FBS) three times and plated on 96-, 12-. or 6-well tissue culture plates (Becton Dickinson Labware, Franklin Lakes, NJ, USA) in DMEM/F12 supplemented with 10% FBS, 10 μg/ml gentamicin (GIBCO), and 25 μg/ml ascorbic acid (Sigma, St. Louis, MO, USA). The purity of the cells was checked by immunofluorescence staining with chondroitin sulfate (CS) (Seikagaku, Tokyo, Japan) and type II collagen (Daiichi Fine Chemical, Toyama, Japan). More than 85% of the cells were positive in both cases (data not shown). Chondrocytes were grown at 37°C in a humidified atmosphere of 5% CO_2 and 95% air, with the medium changed every 2 days. Each of the experiments was performed using the cells of primary culture isolated from ten different patients (age 70–78 years, average 73.4 years).

Immunohistochemistry

Immunofluorescence staining of OA cartilage specimens for TN-C and CS, after antigen retrieval, was performed with 0.01 M citrate buffer at 97°C for 30 min, and sections were incubated with normal goat serum (Dako, Carpinteria, CA, USA) at RT for 30 min. Then they were treated with primary antibodies, mouse monoclonal anti-CS antibody reacted to 4- and 6-sulfates (Seikagaku Corporation, Tokyo, Japan) or rabbit polyclonal anti-TN-C antibody (IBL, Gunma, Japan) at RT overnight. After washes with TBS, the sections were incubated with Alexa Fluor 488-conjugated goat anti-mouse IgG or Alexa Fluor 546-goat anti-rabbit IgG at RT for 3 h. Slides were mounted with Vectashield (Vector Laboratories). All slides were viewed through an epifluorescence microscope equipped with appropriate filters.

Double immunohistochemistry of TN-C and CS was performed. The sections were exposed to the monoclonal anti-CS antibody reacted to 4- and 6-sulfates (Seikagaku) overnight at 4°C and treated with alkaline phosphatase (ALP)-labeled goat anti-mouse IgG Fab′ (Nichirei Biosciences, Tokyo, Japan) for 30 min. The color reaction was achieved with a Fuchsin+ solution (Dako). The immune complexes were removed by treatment with 0.01 N HCl. Then the sections were incubated in 0.04% Proteinase K (Sigma) for 10 min at RT to retrieve the antigens, followed by incubation with monoclonal anti-TN-C antibody (4F10TT; IBL), which is specific to the epidermal growth factor (EGF)-like domain, and reacted with all TN-C variants, overnight at 4°C. The sections were then treated with ALP-labeled goat anti-mouse IgG Fab′ (Nichirei Biosciences) and developed with BCIP/NBT solution (Dako).

Chondroitin sulfate immunoreactivity was red, whereas TN-C immunoreactivity was bluish-violet. Each step was followed by extensive washing in Tris-buffered saline (TBS; pH 7.6). For negative controls, normal mouse IgG was used instead of the first and second primary antibodies.

For double immunohistochemistry of TN-C and PCNA, the sections were treated with a monoclonal anti-PCNA antibody (Dako) and goat anti-mouse IgG Fab′ labeled with peroxidase.[14] The color development was achieved with diaminobenzidine (DAB)/H_2O_2 solution. After the immune complexes were removed by treatment with 0.01 N HCl, they were incubated with 4F10TT antibody and with ALP-labeled goat anti-mouse IgG Fab′, followed by color development with BCIP/NBT. Immunoreactivity of PCNA was brown and that of TN-C was bluish-violet.

To examine the correlation between TN-C staining and chondrocyte proliferation in OA cartilage, three random fields (237 μm^2/field) of each sample from ten articular cartilage samples were observed. Numbers of PCNA strong-positive nuclei and the total number of nuclei were counted in TN-C strong-positive or -negative areas and the labeling indices were provided by determining the percentages of positive nuclei. For negative controls, normal mouse IgG was used instead of the first and second primary antibodies.

Purification of TN-C and its recombinant fragments

TN-C was purified from conditioned medium of U-251 MG human glioma cells by ammonium sulfate precipitation, Sephacryl S-500 gel filtration, and Mono Q ion-exchange chromatography (GE Healthare Bio-Sciences Corp., NJ, USA) as previously described.[6,7]

Cell proliferation assay

Cell proliferation was determined using a colorimetric immunoassay based on the measurement of bromodeoxyuridine (BrdU) incorporated by DNA synthesis. The cells were seeded at 1×10^4 cells/well on 96-well plates (Becton Dickinson Labware). After incubation in a serum-free medium with 0.1% bovine serum albumin (BSA) for 24 h, the cells were treated with 1 μg/ml or 10 μg/ml of TN-C and further cultured for 12 h before the proliferation assay. The BrdU solution was added to a final concentration of 100 μM and the cells were incubated at 37°C for an additional 2 h. The assay was performed using a cell proliferation enzyme-linked immunosorbent assay (ELISA) kit (Roche Diagnostics) according to the manufacturer's instructions. The value obtained from control cells without TN-C treatment was regarded as 100% and the effects of TN-C on cell proliferation were expressed by the relative values.

Proteoglycan content assay

Chondrocytes were cultured at a density of 4×10^4 cells/well in 12-well plates (Becton Dickinson Labware). The cells were cultured at serum starvation with 0.1% BSA for 24 h after chondrocytes reached confluence, and 1 μg/ml or 10 μg/ml of TN-C was added to the wells. After 24 h, the glycosaminoglycan content of the chondrocytes in culture was determined by the dimethylmethylene blue (DMMB ; Polysciences , Warrington, PA, USA) method.[15] In brief, the samples were digested with 20 μg/ml papain in a buffer of 0.1 M sodium acetate, 50 mM ethylenediaminetetraacetic acid (EDTA), and 5 mM L-cysteine at pH 5.53, for 12 h at 60°C, then 200 μl of 16 μg/ml DMMB solution was added to the papain digest of a 150-μl aliquot. The optical densities at 595 and 530 nm were immediately monitored with a spectrophotometer. The ratio of 530/595 nm could determine the glycosaminoglycan amounts. A calibration curve was provided using bovine chondroitin sulfate (ICN Biomedicals, Aurora, OH, USA) as a standard and the amount was normalized by DNA content measured using Hoechst 33258 dye (Polysciences).

RNA extraction and cDNA synthesis

The cells were seeded at 1×10^5 cells/well on 6-well plates (Becton Dickinson Labware). After the cells reached confluence, chondrocytes were treated with different concentrations of TN-C (1 μg/ml or 10 μg/ml) under serum-free conditions with 0.1% BSA. After 12 h, total RNA was isolated using ISOGEN (Nippon-Gene, Toyama, Japan) according to the manufacturer's instructions. Complementary DNA (cDNA) synthesis was performed by oligo $(dT)_{15}$ priming of 1 μg of total RNA using a cDNA synthesis kit (Roche Diagnostics) according to the manufacturer's protocols. TaqMan gene expression assay primer-probe pairs were ordered for the detection of aggrecan (Assay ID. Hs00153936_ml) and glyceraldehyde-3-phosphate dehydrogenase (GAPDH; Assay ID. Hs99999905_ml; Applied Biosystems, Foster City, CA, USA). Quantitative analysis of the cDNA was performed using the ABI Prism 7000 Sequence Detector System (Applied Biosystems) and Taqman Universal polymerase chain reaction (PCR) Master Mix (Roche Diagnosis). The thermal cycling conditions were 50°C for 2 min, 95°C for 10 min, 40 cycles of 95°C for 15 s, and 60°C for 1 min. GAPDH was used as the housekeeping gene for internal control. Aggrecan mRNA levels were normalized by GAPDH levels of each sample. The levels were expressed as an x-fold induction compared with untreated cells.

Statistical analysis

All data were expressed as means ± standard deviation (SD). Numeric data were statistically evaluated by the Kruskal-Wallis test and the Mann-Whitney *U*-test, using StatView software (Abacus Concepts, Berkeley, CA, USA). A *P* value less than 0.05 was considered to be statistically significant.

Results

Immunofluorescence for OA cartilage specimens

Immunolabeling of CS and TN-C was performed in tissue specimens of OA cartilage. The intensity of CS staining was decreased in the superficial zones and increased in the middle zones of the OA specimens (Fig. 1A). TN-C staining was observed in the superficial and middle zones (Fig. 1B). TN-C labeling was detected in matrices surrounding chondrocytes overlying CS-stained area.

Immunohistochemistry of chondroitin sulfate and TN-C in articular cartilage

Normal articular cartilage classified with no evidence of OA, having a total score of 0 to 2 using Mankin's scoring system, was obtained from the femoral condyles of knee joints. A uniform distribution of CS in the pericellular and interterritorial matrices of the middle and deep zones particularly was found. TN-C staining was barely observed in the superficial and upper-middle zones of normal articular cartilage (Fig. 2A, B, C). Sections with total scores of 3 to 6 were classified as mild OA cartilage. An enhancement of TN-C staining was observed at the damaged surface and in the upper-middle zones. In contrast, the intensity of CS staining was decreased in the superficial zones but maintained in TN-C-positive areas of the upper-middle zone (Fig. 2D, E, F). Cartilage samples with total scores from 7 to 10 were ranked as moderate OA. Clefts in the deep zone, some clusters of chondrocytes, and loss of the surface and middle zones were observed. In this stage, CS staining became weaker and marked TN-C staining appeared in the pericellular matrix of chondrocytes in the lower-middle zones. CS staining was partly restricted to the TN-C-positive area (Fig. 2G, H, I). In samples of severe OA, with total scores from 11 to 14, CS staining was found only in the deep zone. TN-C was detected in matrices surrounding the chondrocytes of deep zones overlying CS staining (Fig. 2J, K, L). The control sections showed no staining (data not shown).

TN-C expression and chondrocyte proliferation in articular cartilage

In normal cartilage, TN-C staining and PCNA-positive nuclei were hardly observed (Fig. 3A). In the TN-C-positive area of OA cartilage, PCNA-labeled nuclei were significantly more frequent than in the negative area (Fig. 3B, C). Labeling indices of PCNA in TN-C-positive areas were significantly higher than those in the -negative areas ($p < 0.01$) (Table 1). The control slides showed no staining (data not shown).

Proliferation of cultured chondrocytes after TN-C treatment

Compared with the control cells without TN-C, BrdU incorporation of the cells treated with 10 μg/ml TN-C was significantly increased ($P < 0.01$), while that of the cells treated with 1 μg/ml of TN-C was not (Table 2).

Table 1. Labeling index of PCNA in TN-C expression

	TN-C staining	
	(−)	(+)
Labeling index (%)	4.7 ± 4.4	41.0 ± 10.5*

*$P < 0.01$ compared with TN-C negative areas
Results are means ± standard deviation
PCNA, proliferating cell nuclear antigen; TN-C, tenascin-C

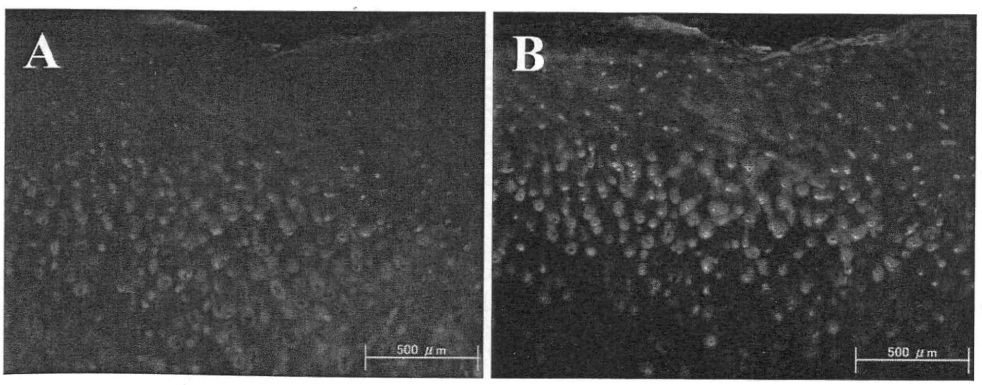

Fig. 1A,B. Photomicrographs are representative of osteoarthritis (OA) articular cartilage showing immunofluorescence staining for chondroitin sulfate (CS, **A**) and tenascin-C (TN-C, **B**). *Bars*, 500 μm for **A** and **B**

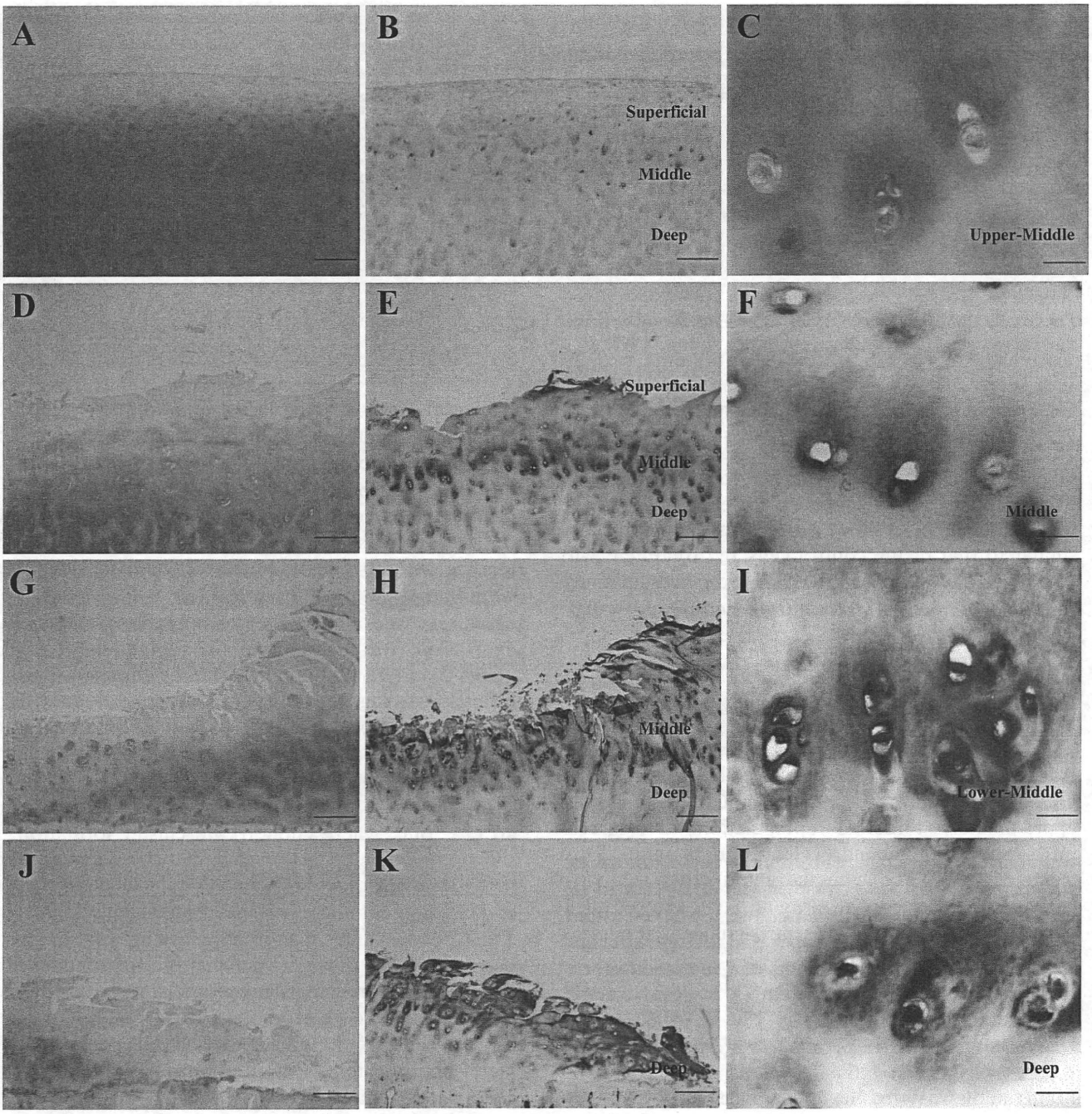

Fig. 2A–L. Photomicrographs are representative of articular cartilage stained with safranin O (**A**, **D**, **G**, and **J**), and double-immunostained with anti-TN-C and anti-CS antibodies (**B**, **C**, **E**, **F**, **H**, **I**, **K**, and **L**). *Bars*, 500 μm for **A**, **B**, **D**, **E**, **G**, **H**, **J**, and **K**; 50 μm for **C**, **F**, **I**, and **L**

Table 2. Proliferation, proteoglycan (PG) content, and aggrecan mRNA in cultured chondrocytes after TN-C treatment

TN-C (μg/ml)	0 (control)	1	10
BrdU incorporation (%)	100.0 ± 19.8	104.9 ± 46.1	159.8 ± 35.0*
PG content (μg/μg DNA)	4.2 ± 1.7	4.0 ± 1.6	6.0 ± 1.4**
Relative aggrecan mRNA levels	1.00 ± 0.18	1.35 ± 0.69	3.25 ± 1.32***

* $P < 0.01$ compared with control; ** $P < 0.05$ compared with control; *** $P < 0.01$ compared with control
Results are means ± standard deviation
BrdU, bromodeoxyuridine

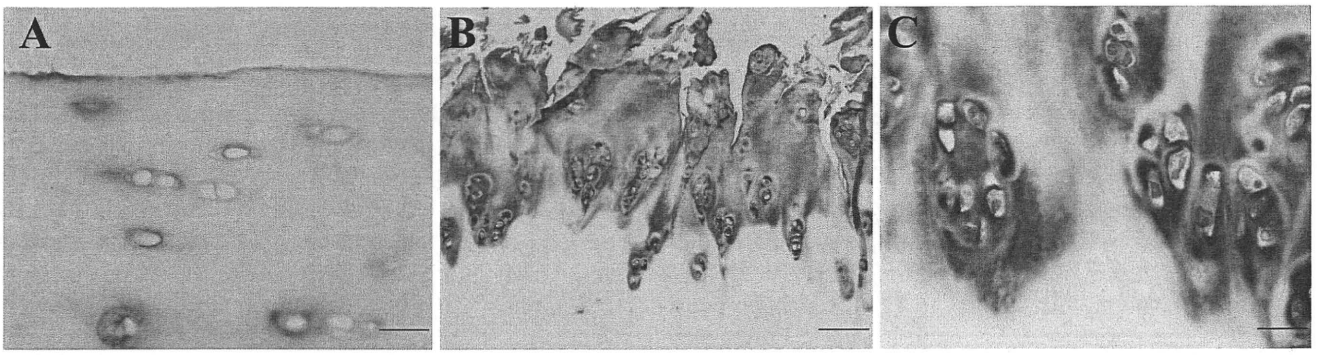

Fig. 3A,B. Photomicrographs are representative of articular cartilage double-immunostained for TN-C and proliferating cell nuclear antigen (PCNA). *Bars*, 50 μm for **A** and **C**, 200 μm for **B**

Glycosaminoglycan content of chondrocyte culture after TN-C treatment

Glycosaminoglycan content was corrected by the DNA content of each culture. Whereas the effect of treatment with 1 μg/ml TN-C showed no statistical significance, similar to that of the control cells, the treatment with 10 μg/ml TN-C significantly enhanced glycosaminoglycan accumulation in chondrocyte culture ($P < 0.05$; Table 2).

Aggrecan mRNA levels in cultured chondrocytes after TN-C treatment

Aggrecan transcripts were quantified by real-time PCR. Quantitative analysis by real-time PCR demonstrated approximately threefold upregulation of aggrecan mRNA levels in chondrocytes after 10 μg/ml TN-C treatment compared with untreated cell levels ($P < 0.01$), while treatment with 1 μg/ml TN-C showed slight upregulation, but there was no significant difference (Table 2).

Discussion

In this study, we noted the appearance of TN-C staining and its increase in the pericellular and interterritorial matrices of the middle and deep zones as well as fibrillated cartilage. Several studies have also shown increased TN-C labeling in osteoarthritic conditions compared with normal cartilage.[9,10] The increase of TN-C surrounding chondrocytes suggested that the cells themselves could produce TN-C in OA cartilage. The expression of TN-C, as well as aggrecan, in chondrocytes was regulated by interleukin (IL)-1β and was increased in OA cartilage.[9] In addition, mechanical loading is well known to regulate TN-C expression.[16] Physiologically relevant stress responses could be related to the expression of TN-C in wounds or around tumors.[17] We found enhanced TN-C labeling in parallel with decreased CS staining in damaged OA cartilage in some sections. CS is a sulfated glycosaminoglycan found in articular cartilage and is composed of repeating disaccharide units of glucuronic acid and galactosamine. Articular cartilage resists compressive force because of its capacity for binding water to the CS domains of aggrecan. Therefore, CS loss may result in increased mechanical loading of chondrocytes, followed by the upregulation of TN-C expression. We suggest that the regulation of TN-C increase and CS loss is performed by common mechanisms in cartilage. Furthermore, the present study also showed the colocalization of CS with TN-C staining in cartilage matrix around chondrocytes in part of the survival zones in the damaged cartilage.

In the middle to deep zones of articular cartilage in an OA joint, where chondrocyte cluster formation is shown, this being a major characteristic phenotype in the diseased cartilage, we found that the labeling indices of PCNA in chondrocytes were significantly higher in TN-C-positive areas than in -negative areas. It has also been found that TN-C-rich foci were associated with PCNA immunoreactivity in smooth muscle cells.[18] We also demonstrated a promoting effect of TN-C on the proliferation of cultured chondrocytes. TN-C may stimulate chondrocyte proliferation for repair in the pathogenesis of OA cartilage.

Our in vitro studies suggest that TN-C upregulates the mRNA expression of aggrecan in chondrocytes and increases the amount of glycosaminoglycan in the culture. Aggrecan consists of a long protein core to which more than 100 glycosaminoglycan chains are attached. Increases in aggrecan gene expression are correlated with increases in secreted proteoglycan synthesis. The components of proteoglycan are produced separately by the chondrocytes and extruded into the pericellular matrix as aggrecan. In OA cartilage, increased synthesis of aggrecan induced by TN-C stimulation could partly explain their colocalization. Chondrocytes are thought to be surrounded by a specialized

microenvironment known as a chondron. TN-C appears to be an important constituent of this microenvironment.[19] The chondron has been shown to represent a key site of degradative matrix changes in OA cartilage. Aggrecan is a major component of the chondron and an important factor in the retention of collagen within cartilage.[20] Day et al[21] showed that the aggrecan G3 domain could bind to TN-C and that alternative splicing of the domain influenced the binding interaction. The splice variant with the highest affinity to TN-C has been confirmed to be expressed by chondrocytes. From our immunohistochemical findings, showing that CS staining was decreased but partly maintained in TN-C-positive areas surrounding chondrocytes in OA cartilage, we speculate that the molecular interaction of TN-C could maintain the accumulation of aggrecan with a CS side chain in the chondron and modulate the anchoring of the chondrocytes to the matrix. Furthermore, in normal deep cartilage, previous studies have demonstrated that chondrocytes in deep zones are more active in glycosaminoglycan synthesis than superficial chondrocytes, and TN-C could be found in the deep areas of some normal cartilage.[9,22,23] It may be that the chondrocytes obtained from zones that maintained both CS and TN-C staining or those obtained from deep almost intact areas in human OA cartilage may have sensitized TN-C responsiveness.

It is known that TN-C is expressed during chondrogenesis within the embryo, and in vitro studies were devised to investigate the function of TN-C during chondrogenesis.[24] TN-C may be correlated to the development of permanent articular cartilage composed of specific matrix. Also, matrix protein such as aggrecan is required for repair in osteoarthritic cartilage, and our study, by the double-immunostaining and articular chondrocyte culture experiments, indicated that TN-C could produce cartilaginous matrix during OA disease. However, it was reported that transgenic mice without distributed TN-C gene production developed normally.[25] Other factors may replace or supplement TN-C action. A previous study has shown that fibronectin appears diminished in the repair of epithelial tissue in mice lacking TN-C.[26] We also observed that myocardial tissue repair was partly abnormal in TN-C-deficient mice, and it is not known whether cartilage repair occurs during the disease progression in TN-C knockout mice.[7]

A previous in vivo study showed that 400 ng/ml TN-C did not trigger adverse reactions within joint cavities.[27] The repair tissue formed within defects treated with TN-C had more fibrous components. It was surprising that TN-C failed to elicit chondrogenesis in that experiment, but the concentration of TN-C was lower than the 10 μg/ml used in our study to induce chondrocyte proliferation, glycosaminoglycan production, and aggrecan mRNA expression. The influence of 10 μg/ml TN-C requires further study in vivo. Furthermore, it is considered that TGF-β conducts cartilage repair in OA, and it has been well studied that these kinds of factors also induce TN-C expression in various kinds of cells.[28–30] The coordination of TN-C with these molecules may develop a microenvironment of chondrocytes for cartilage repair in vivo. The present study, using an expression pattern and gain-of-function type in vitro experiment, showed some association of TN-C with cartilage repair. To establish a cause-and-effect relationship, however, it is necessary to perform loss-of-function type experiments using small interfering (si)RNA for TN-C in vitro and using TN-C-knockout animals. In the future, TN-C might be used for repairing OA cartilage.

Conclusions

TN-C could be one of the key molecules for regulating chondrocyte proliferation and forming cartilage matrices in OA cartilage. Further investigation is needed to clarify the biological functions of TN-C in articular cartilage disease in vivo.

None of the authors of this manuscript has received any type of support, benefits, or funding from any commercial party related directly or indirectly to the subject of this article.

References

1. Buckwalter JA, Martin JA. Osteoarthritis. Adv Drug Deliv Rev 2006;58:150–67.
2. Jenniskens YM, Koevoet W, de Bart AC, Weinans H, Verhaar JA, Jahr H, et al. Biochemical and functional modulation of the cartilage collagen network by IGF1, TGFbeta2 and FGF2. Osteoarthritis Cartilage 2006;14:1136–46.
3. Chiquet-Ehrismann R. Tenascins, a growing family of extracellular matrix proteins. Experientia 1995;51:853–62.
4. Chiquet-Ehrismann R, Mackie EJ, Pearson CA, Sakakura T. Tenascin: an extracellular matrix protein involved in tissue interactions during fetal development and oncogenesis. Cell 1986;47: 131–9.
5. Yoshida T, Matsumoto E, Hanamura N, Kalembeyi I, Katsuta K, Ishihara A, et al. Co-expression of tenascin and fibronectin in epithelial and stromal cells of benign lesions and ductal carcinomas in the human breast. J Pathol 1997;182:421–8.
6. Yoshida T, Yoshimura E, Numata H, Sakakura Y, Sakakura T. Involvement of tenascin-C in proliferation and migration of laryngeal carcinoma cells. Virchows Arch 1999;435:496–500.
7. Tamaoki M, Imanaka-Yoshida K, Yokoyama K, Nishioka T, Inada H, Hiroe M, et al. Tenascin-C regulates recruitment of myofibroblasts during tissue repair after myocardial injury. Am J Pathol 2005;167:71–80.
8. Mackie EJ, Murphy LI. The role of Tenascin-C and related glycoproteins in early chondrogenesis. Microsc Res Tech 1998;43: 102–10.
9. Pfander D, Heinz N, Rothe P, Carl HD, Swoboda B. Tenascin and aggrecan expression by articular chondrocytes is influenced by interleukin 1β: a possible explanation for the changes in matrix synthesis during osteoarthritis. Ann Rheum Dis 2004;63:240–4.